



Contents lists available at ScienceDirect

Estuarine, Coastal and Shelf Science

journal homepage: www.elsevier.com/locate/ecss

Modeling the dynamics and export of dissolved organic matter in the Northeastern U.S. continental shelf

J.N. Druon^{a,*}, A. Mannino^a, S. Signorini^a, C. McClain^a, M. Friedrichs^b, J. Wilkin^c, K. Fennel^d

^a NASA Goddard Space Flight Center, Ocean Biology Processing Group, Code 614.8, Greenbelt, MD 20771, USA

^b Virginia Institute of Marine Science, The College of William & Mary, Route 1208, Great Road, Gloucester Point, VA 23062-1346, USA

^c Rutgers University, 71 Dudley Road, New Brunswick, NJ 08901-8521, USA

^d Dalhousie University, Department of Oceanography, Halifax, NS, Canada B3H 4J1

ARTICLE INFO

Article history:

Received 13 July 2009

Accepted 18 May 2010

Available online 1 June 2010

Keywords:

dissolved organic matter
dissolved organic carbon
dissolved organic nitrogen
transport
carbon burial
modeling
USA
Mid-Atlantic Bight

ABSTRACT

Continental shelves are believed to play a major role in carbon cycling due to their high productivity. To improve our understanding of carbon dynamics on continental margins, a dissolved organic matter (DOM) model was developed and imbedded within an existing coupled ocean circulation–biogeochemical model of the U.S. East coast. A model simulation with the DOM module was compared with the reference model (without the DOM module) to illustrate the role of DOM dynamics in coastal ocean biogeochemical cycling. Model results reveal that the progressive release of dissolved organic nitrogen (DON) in the ocean's upper layer during summer increases the regenerated primary production by 30–300%, which, in turn, enhances the dissolved organic carbon (DOC) production mainly from phytoplankton exudation in the upper layer and solubilization of particulate organic matter (POM) deeper in the water column. This analysis suggests that DOM is a necessary component for representing ecosystem functioning and organic fluxes in models because DOM (1) is a major organic pool directly related to primary production, (2) decouples partially the carbon and nitrogen cycles (through carbon excess uptake, POM solubilization and DOM mineralization) and (3) is intimately linked to the residence time of water masses for its distribution and export. The seasonally produced DOC on the shelf can be exported to the open ocean by horizontal transport at comparable rates ($1\text{--}2 \text{ mol C m}^{-2} \text{ yr}^{-1}$) to particulate organic carbon burial in the southern U.S. Mid-Atlantic Bight (MAB).

© 2010 Elsevier Ltd. All rights reserved.

1. Introduction

Dissolved organic matter (DOM) has received increasing attention over the past few decades because dissolved organic carbon (DOC) represents by far the largest pool of organic carbon in the ocean. DOC export from the surface global ocean is estimated at 20% of total organic carbon flux to the deep ocean (Six and Maier-Reimer, 1996; Hansell, 2002), which represents an important control on atmospheric carbon dioxide levels (i.e. the biological pump). Particulate organic carbon (POC), which accounts for 80% of the organic carbon export in the open ocean, is mainly recycled on the shelf and fuels the DOC pool. If residence times of shelf waters are shorter than the lifetime of much of the seasonally produced DOC, the horizontal DOC flux could represent

the main contribution to the export of organic carbon to the open ocean and exceed sinking POC fluxes (Bauer and Druffel, 1998).

DOM is believed to play an important role in carbon and nitrogen cycling from regional to global scales. Models have included DOM to study eutrophicated (Lancelot et al., 2005), eutrophic (upwelling, Ianson and Allen, 2002), mesotrophic (Anderson and Williams, 1998; Fasham et al., 1999) and oligotrophic (Anderson and Pondaven, 2003; Raick et al., 2005) regional systems and the global ocean (Popova and Anderson, 2002). Fasham et al. (1999) demonstrated that accounting for DOC is essential for euphotic ecosystem models and development of a carbon budget. Because DOC and DON dynamics are partially decoupled (e.g. carbohydrate production, mineralization rates), these models explained important deviations from the Redfield ratio in terms of productivity and export fluxes, and sustained nutrient-based primary production through DON mineralization and atmospheric inputs (Seitzinger and Sanders, 1999).

The Mid-Atlantic Bight (MAB) is the central region of the eastern U.S. continental shelf characterized by high rates of primary

* Corresponding author at: Present address: Joint Research Centre of the European Commission, Institute for the Protection and Security of the Citizen, Maritime Affairs Unit, Via Fermi, TP 051, 21027 Ispra (VA), Italy.
E-mail address: jean-noel.druon@jrc.ec.europa.eu (J.N. Druon).

productivity and strong residual circulation. This region is thus a potential area of organic carbon export to the open ocean. The DOC pool in the MAB is one to three orders of magnitude larger than the POC pool (Bauer et al., 2001). The hydrography and circulation of the MAB is well studied (Biscaye et al., 1994) with a general north–south flow from Georges Bank to Cape Hatteras. The greatest inflow of water to the MAB (0.4 Sv, Beardsley and Boicourt, 1981) is from Georges Bank. This flow represents the southern extension of the Labrador Current with averaged (total) DOC concentrations between 72 and 75 mmol m⁻³ (Vlahos et al., 2002). In the southern MAB near Cape Hatteras, the warm and salty water of the Gulf Stream has a major impact on the flow and exchange of water on the shelf and slope. Although the mean circulation is along-shelf in the southwestward direction, cross-shelf exchanges due to frontal instabilities and eddies displace significant portions of the shelf water to the open ocean north of Cape Hatteras (Biscaye et al., 1988). The freshwater inflow (0.005 Sv) to the MAB is about 1% of the total water inflow (Beardsley and Boicourt, 1981), but represents a significant input of total DOC with mean concentrations of 200–400 mmol C m⁻³ in the mid-Bay of the Chesapeake Bay (data from the Chesapeake Bay Program, <http://www.chesapeakebay.net/wquality.htm>) throughout the year and 90–190 mmol C m⁻³ in the mouths of the MAB estuaries (Sharp et al., 1982; Fisher et al., 1998; Bates and Hansell, 1999; Harvey and Mannino, 2001; Taylor et al., 2003). Strong gradients in DOM concentration exist between estuarine, shelf and open ocean waters (Hopkinson et al., 2002; Vlahos et al., 2002). The DOM concentrations on the shelf are elevated compared to the open ocean and contain a larger labile fraction and younger DOC (Bauer et al., 2002) than DOM in deep slope waters, where carbon is more refractory and enriched relative to nitrogen and phosphorus (Hopkinson et al., 2002). Because half-lives of the labile DOM pool are on the order of shelf-water residence time (~100 days), a substantial pool of DOM that is depleted in nitrogen and phosphorus relative to carbon remains and a net export of DOC to the open ocean can occur by advective and eddy diffusive processes (Hopkinson et al., 2002). A DOC budget study based on field measurements estimated a total export from the MAB shelf to the open ocean of 18.7–19.6 Tg C yr⁻¹ (Vlahos et al., 2002). To our knowledge, there has been no attempt to model the DOC dynamics and fluxes in the MAB.

The goal here is to model and evaluate the impact of DOM to carbon cycling in the MAB and to estimate the horizontal export of semi-labile DOC to the open ocean. A model simulation with the DOM module was compared with the reference model (without the DOM module) to illustrate the role of DOM dynamics in coastal ocean biogeochemical cycling. This paper is organized as follows. After a brief description of the coupled physical–biogeochemical model, a brief overview of the DOM module is presented (Section 2, and detailed in the Appendix), the model validation and results are described (Section 3) and discussed (Section 4) with a focus on DOM dynamics and carbon export to the open ocean.

2. Model description

2.1. The physical model

The three-dimensional ocean circulation model (ROMS, Regional Ocean Modeling System version 3) extends across the Northeast North American (NENA) shelf including the Scotian shelf, the Gulf of Maine, the MAB, the South Atlantic Bight (SAB), the Eastern Gulf of Mexico and the adjacent deep sea (Fig. 1). The focus of this paper is on the continental margin of the MAB and Georges Bank regions (Fig. 1). The NENA model is nested within a North

Atlantic (NA) model in order to capture large circulation features and variability such as the Labrador Current, the Gulf Stream and associated subtropical gyre circulation.

ROMS (Haidvogel et al., 2000, 2008) is a model widely used for shelf circulation and coupled physical–biological applications (e.g. Dinniman et al., 2003; Marchesiello et al., 2003; Peliz et al., 2003; Fennel et al., 2006; Wilkin, 2006). The application on the NENA domain uses a 10-km horizontal resolution and 30 terrain-following vertical levels stretched to give high resolution in surface and bottom boundary layers. This resolution is sufficient to capture the dominant dynamics governing shelf-wide circulation. Open boundary temperature, salinity and sub-tidal frequency velocity are taken from 3-day averages of the Hybrid Coordinate Ocean Model data assimilation product developed as part of the Global Ocean Data Assimilation Experiment North Atlantic Basin ‘best-estimate’ analysis for 2003–2006. Tides have been introduced at the boundary using harmonic data from the Oregon State University Topex/Jason altimeter data inversion and a surface gravity wave radiation scheme (Flather, 1976). Air–sea heat and momentum fluxes are computed using bulk formulae (Fairall et al., 2003) applied to model sea surface conditions, and air temperature, pressure, humidity and winds from daily average National Center for Environmental Prediction re-analysis fields. Vertical turbulent mixing closure uses the parameterization of Mellor and Yamada (1982) and Warner et al. (2005). Coastal freshwater inputs are applied using USGS river flow data.

This model exhibits recognized features of local and remotely forced circulation on the shelf and slope. These include wind-driven upwelling in the MAB, buoyancy-driven river plumes, tidal mixing and tidal residual mean currents on Georges Bank, southwestward mean flow in the MAB and retention of passive particles in the shelf-slope front. In addition the model captures interactions of Gulf Stream warm rings with the New England slope (Hofmann et al., 2008). The simulations described below use a higher background value for diffusivity (10⁻⁵ m² s⁻¹) than in Fennel et al. (2006) (10⁻⁶ m² s⁻¹) to compensate for the lack of secondary mixing processes such as internal waves and sub-grid turbulent diffusion. Similar background levels of diffusivity were shown to be necessary to reproduce the vertical temperature field and have been used in other model applications as well (10⁻⁵ m² s⁻¹, Kantha and Clayson, 1994, and 2 × 10⁻⁵ m² s⁻¹, Ledwell et al., 1993).

2.2. The biogeochemical model with DOM

A general overview of the biogeochemical model schematic is presented in Fig. 2 and the full details of the DOM processes and governing equations including the semi-labile DON and DOC are presented in the Appendix. The semi-labile DOC and DON were added as state variables to an existing nitrogen-based model (Fennel et al., 2006) and inorganic carbon component (Fennel et al., 2008). The nitrogen model includes eight state variables: nitrate (NO₃), ammonium (NH₄), phytoplankton (Phy), semi-labile DON (named hereafter DON), zooplankton (Zoo), small and large detritus (SDetN and LDetN) and phytoplankton chlorophyll (Chl). The nitrogen-cycling formulations used are the same as those in Fennel et al. (2006), except for the resuspension and burial of POM (see Appendix and Table A2) which were added to meet the requirements of the DOM equations at the seabed interface. The carbon model includes dissolved inorganic carbon (DIC), semi-labile DOC (named hereafter DOC) and small and large detritus (SDetC and LDetC). Two terms describe the semi-labile DOC exudation by phytoplankton in the model. The nutrient-based release reflects the healthy phytoplankton exudation of semi-labile DOC, and the semi-labile DON exudation

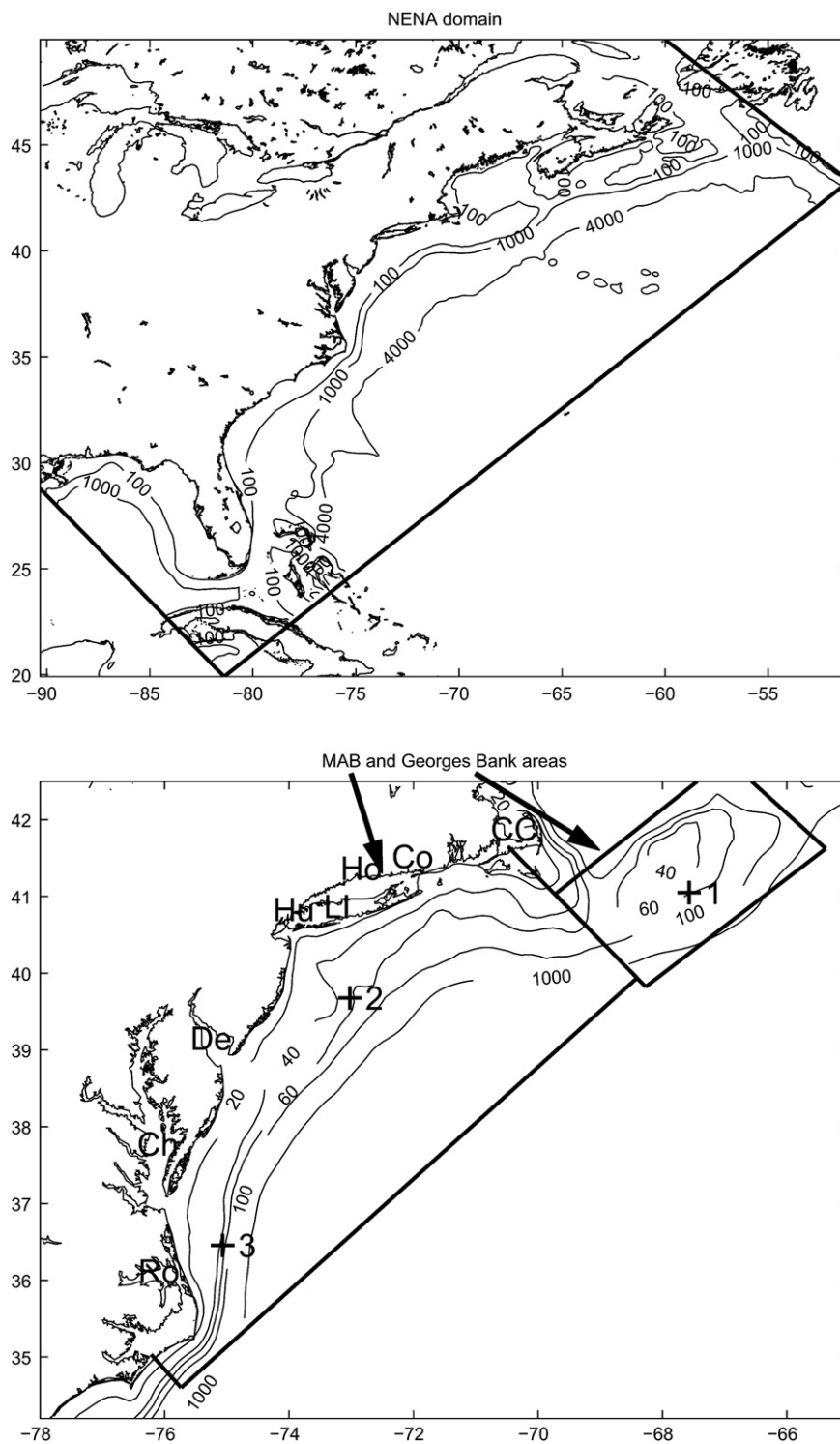


Fig. 1. Geographical location and bathymetry (in meters) of the Northeast North Atlantic (NENA) model domain (upper graph) and details of the Middle Atlantic Bight (MAB) and Georges Bank regions (bottom graph). The three numbered stations cited in the text are also shown. The locations cited in the text are: 'CC' Cape Cod, 'Co' Connecticut River, 'Ho' Housatonic River, 'LI' Long Island, 'Hu' Hudson River, 'De' Delaware Bay, 'Ch' Chesapeake Bay, 'Ro' Roanoke River.

follows the Redfield ratio. The carbon excess-based release represents the carbohydrate over-production by nutrient-stressed cells. The carbon excess uptake represents dissolved inorganic carbon taken up by phytoplankton under nutrient limitation and released as DOC. Phytoplankton and zooplankton in carbon units are expressed using the nitrogen unit equation and their specific C–N ratio (CN_P and CN_Z respectively); thus no

explicit equations are required (see Appendix). The DIC dynamics and air–sea exchange of carbon dioxide are described in Fennel et al. (2008).

2.2.1. Semi-labile DOC and DON lability

The definition of the DOC and DON pools may vary significantly between authors, therefore a definition is provided here.

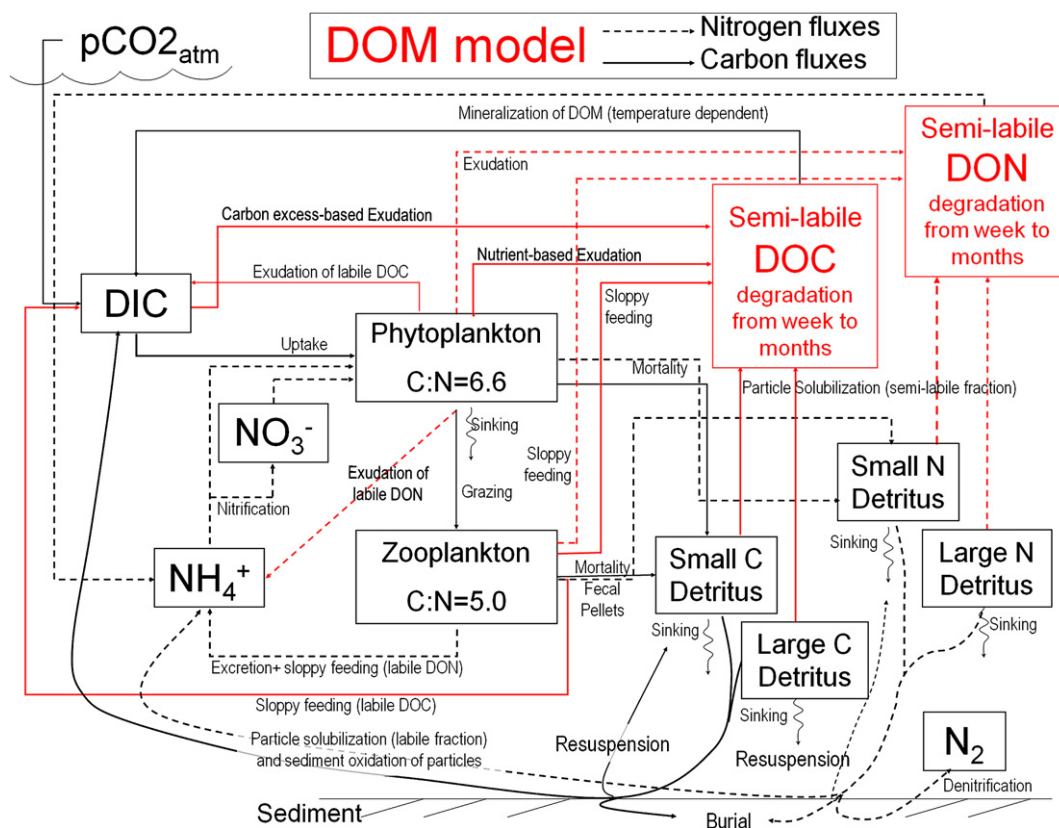


Fig. 2. Flow diagram of the ecosystem model with the dissolved organic matter (DOM) module including the carbon (solid) and nitrogen (dash) cycles. The DOM sink and source fluxes are highlighted in red.

The DOM pool is generally divided into labile, semi-labile and refractory pools although a continuum of biological lability exists between these categories (Amon and Benner, 1996). Highly variable decomposition (or turnover) rates of DOC were measured for surface and bottom waters of the MAB (Hopkinson et al., 2002). The refractory pool has a very long turnover time (several thousand years on average, Druffel et al., 1992; Santschi et al., 1995), and its concentration is relatively constant in the surface ocean at the yearly time scale. Although refractory DOM represents on average 70% of the total DOC pool and 61% of the total DON pool in shelf and slope waters of the MAB (Hopkinson et al., 2002), the model does not take into account its variability since this study concentrates on the seasonal production of DOM. The labile material is defined here as having a turnover time scale of a few days to hours. Since it is mineralized in a few days within the 10 km-grid box of the model, the labile DOM is directed to the dissolved inorganic compartments (DIC and NH₄). The semi-labile fraction simulated by the model has a turnover time of one week to several months (due to a temperature dependency), which is on the order of the shelf residence time in the MAB (~100 days). As such this defined semi-labile DOM can therefore be efficiently exported to the open ocean by horizontal transport.

2.3. Initial and boundary conditions

Initial and boundary conditions for nitrate were derived using polynomial approximations that predict nitrate concentration from temperature using the NODC World Ocean Database 2001 (Fennel et al., 2006). The semi-labile DOC and DON boundary conditions are constant and set to 1.0 mmol m⁻³ and

0.15 mmol m⁻³ respectively. This approximation does not affect the MAB area because it is far enough from the boundary limits of NENA (Fig. 1) to lose its memory, i.e. the time required to transport water masses from the boundary limit to the MAB is significantly higher than the semi-labile DOM half-life. The same reasoning was applied to all other biological state variables with boundary conditions set to small background values. Monthly climatology for river flow, nitrate, and ammonium were derived from the U.S. Geological Survey monitoring database. The MAB receives a large supply of freshwater from the Hudson, Delaware and Chesapeake estuaries that carries high loads of DOC. Much of this DOC is believed to be of terrestrial origin, consisting of mostly refractory organic matter that can be transported across the shelf and into the open ocean (Aluwihare et al., 2002; Bauer et al., 2002). Although the semi-labile fraction is believed to be small, the main input of freshly produced DOM to the MAB is from production within the estuaries. Since the boundary conditions for the Chesapeake Bay and Delaware Bay are located in the mid and upper bay respectively, a polynomial fit is applied to the DOC data available in these areas from the Chesapeake Bay Program database (<http://www.chesapeakebay.net/wquality.htm>) and other sources (Jon Sharp, pers. comm.). A dampened seasonal pattern is applied with a minimum DOC value in March and a maximum value in early October with a mean of 297 ± 14 mmol m⁻³. A small fraction (10%) represents the semi-labile DOC and is used as a boundary condition for rivers. The boundary condition for semi-labile DON is derived using a Redfield C–N ratio, which approximately characterizes freshly produced DOM (i.e. the semi-labile fraction). The river boundary condition for phytoplankton biomass and chlorophyll is set to background values of 1.8 mmol N m⁻³ and 6.0 mg Chl m⁻³, respectively.

3. Model results

A spin up of seven months is conducted on the NENA domain to initialize the biogeochemical model (June 2003) for the year 2004. The results of twin simulations – with and without the DOM – are discussed in the following subsections.

3.1. Vertical and seasonal distribution of DOM

A station chosen for the representativeness of the vertical and seasonal DOM processes in the southern MAB shelf is discussed (station 3, Fig. 1) and compared to stations in the central MAB and Georges Bank areas (Fig. 3). The bulk of semi-labile DON is formed during the late-bloom periods at the 3 stations with a maximal value of 3 mmol m^{-3} . This value is in agreement with the observed seasonal increase of $2\text{--}5 \text{ mmol m}^{-3}$ (Hopkinson et al., 1997). The semi-labile DOC pool builds up rapidly on the shelf during the decay phase of the spring bloom with values up to 55 mmol m^{-3} at station 2 and 3 and 35 mmol m^{-3} at station 1. While this freshly produced DOC pool decreases in June and July down to 15 mmol C m^{-3} at station 3 following the decline of the subsurface biomass (Fig. 4b), it is largely maintained during summer in the Central MAB and even increased on Georges Bank (Fig. 5).

The primary production at station 3 is characterized by a nitrate-sustained production at the subsurface in summer. Although the water depth is 46 m, station 3 is near the shelf break and episodically under the influence of the Gulf Stream. A nitrate concentration of 5 mmol m^{-3} is encountered at the depth of the 10% isolume during that period following an intrusion of the Gulf Stream as was suggested in other studies (Schollaert et al., 2003) and observed in July 1996 (Redalje et al., 2002). The most important period of nutrient uptake occurs during summer between the mixed layer depth and the depth of the 10% isolume, with values up to

$0.8 \text{ mmol NO}_3 \text{ m}^{-3} \text{ d}^{-1}$ and $0.5 \text{ mmol NH}_4 \text{ m}^{-3} \text{ d}^{-1}$. A peak of DOC up to 23 mmol m^{-3} is observed in August in relation with the Gulf Stream intrusion (Fig. 4).

The annual new production at station 3 is 46% of the nitrogen-based production, compared to 36% at station 2 where the Gulf Stream has less influence and 41% at the well-mixed tidal-driven station 1. The carbon excess uptake at station 3 of $30 \text{ g C m}^{-2} \text{ yr}^{-1}$ represents 12% of total primary production (14% at station 2 and 6% at the nutrient-rich station 1). This 'extra' carbon uptake occurs at a shallower depth than the nutrient uptake, where the gradients of biomass and light intersect.

Fig. 5a shows the seasonal variability of the semi-labile DOC concentration at the surface in the MAB and Georges Bank. The peak in semi-labile DOC occurs in spring in the inner MAB ($\sim 65 \text{ mmol m}^{-3}$) and in summer on Georges Bank with the highest value in the shallowest area (from 30 to 50 mmol m^{-3}). The slope off the MAB and Georges Bank between 100 and 1000 m shows a local maximum concentration in spring in relation with primary productivity.

The model exhibits a stable and minimum C–N ratio of DOM during the growth phase of the spring bloom and an increasing ratio during the stationary and decay phases. The C–N ratio (atoms) of DOM during the post-bloom increases from 10.5 to 14.5 at station 1, 12.5 to 21.5 at station 2 and from 12.5 to 18.5 at station 3 in agreement with previous measurements (between 10 and 25, Benner et al., 1992).

3.2. Horizontal DOM distribution and model evaluation

The general distribution of total DOC concentration in surface waters shows an increase from northeast to southwest, and from offshore to inshore (Vlahos et al., 2002). These gradients arise from the production and accumulation of total DOC concentration on the

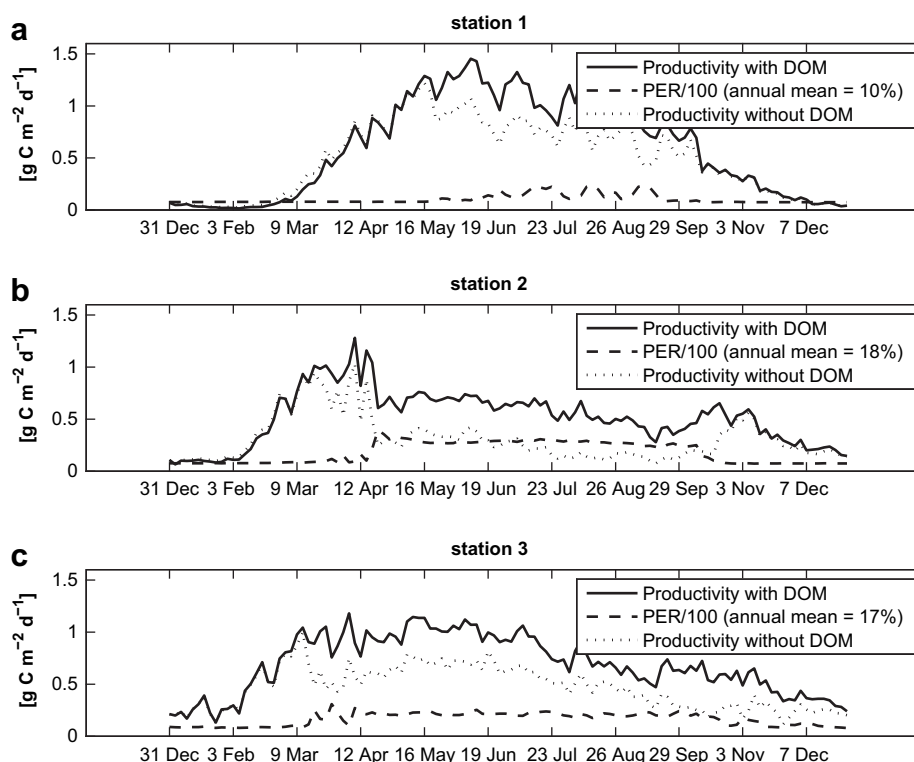


Fig. 3. Simulated daily vertically integrated primary production results for twin experimental model runs with DOM module (solid) and without DOM (dots) and percentage of extracellular release (PER, dash) of dissolved organic carbon (DOC) at (a) a 59 m depth station on Georges Bank (station 1, see Fig. 1 for position), (b) a 55 m northern MAB station (station 2) and (c) a 46 m southern MAB station (station 3). PER represents the percentage of organic carbon exuded by phytoplankton as DOC relative to total primary production.

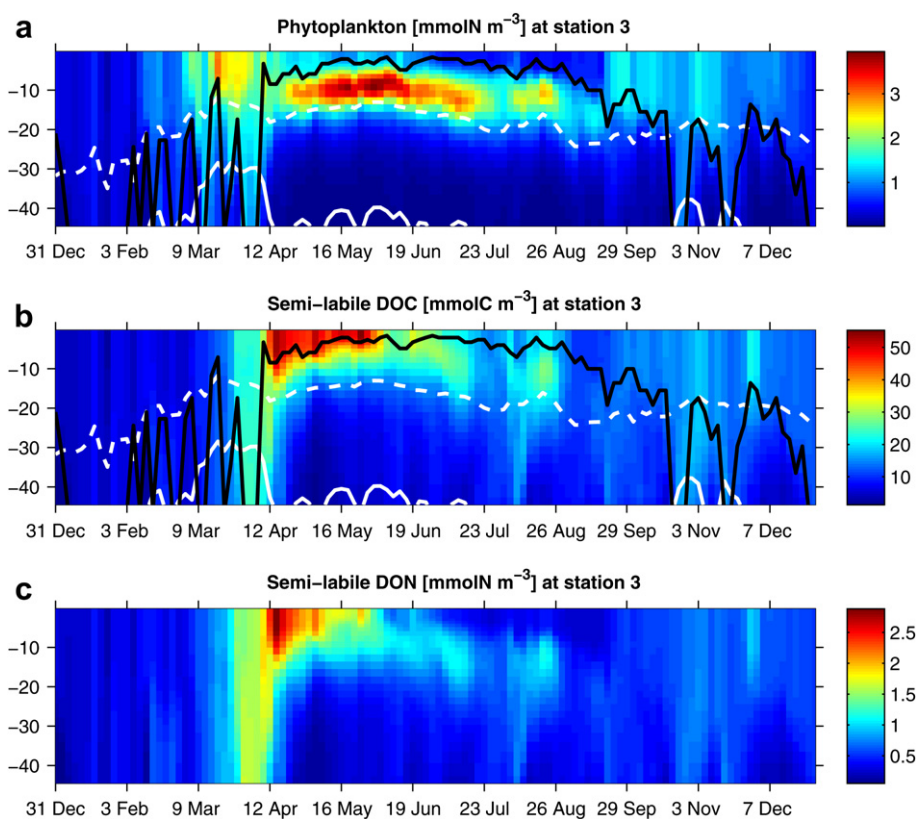


Fig. 4. Seasonal profiles of (a) phytoplankton biomass (mmol N m^{-3}), (b) semi-labile DOC (mmol C m^{-3}) and (c) semi-labile dissolved organic nitrogen (DON, mmol N m^{-3}) simulated by the model at station 3 (southern mid-shelf MAB). The mixed layer depth (solid black) and the depth of the 10% (dash white) and 1% (solid white) isolume are also shown.

shelf as a result of primary production and river inputs to the southwestward flowing water mass (Vlahos et al., 2002; Mannino et al., 2008). The validation of the modeled semi-labile DOC is complicated by the different quantity measured in the field (total DOC) that includes the labile and refractory fractions. Furthermore due to the particularly coarse model resolution in the estuary areas, we have less confidence in the simulated estuarine production. The DOC decomposition study of Hopkinson et al. (2002) for near-surface waters of the southern MAB showed a degradable DOC pool of $28\text{--}36 \text{ mmol C m}^{-3}$ in March 1996 and $40\text{--}49 \text{ mmol C m}^{-3}$ in August 1996 (sum of two DOC components with half-lives of 1–4 days and 16–34 days for stations T5S4 and T6S1). Assuming that refractory DOC represents on average 70% of the total DOC (Hopkinson et al., 2002), we can estimate the semi-labile DOC concentration as 30% of total DOC measured. Applying the DOC measurements from Vlahos et al. (2002) for the MAB and Georges Bank yields semi-labile DOC concentrations of $20.7\text{--}51 \text{ mmol C m}^{-3}$ in April 1994, $15.2\text{--}53.1 \text{ mmol C m}^{-3}$ in March 1996 and $20\text{--}52.3 \text{ mmol C m}^{-3}$ in August 1996. These values are generally consistent with the model results (Fig. 5a). The seasonal mean of semi-labile DOC for 2004 was also estimated from satellite-derived (SeaWiFS) total DOC (Fig. 5b; Mannino et al., 2008) applying the 70% cut. Taking into account the high spatial, seasonal and interannual variability, the semi-labile DOC on the shelf is in general agreement with the field and satellite-derived estimations, especially regarding the inner–outer shelf gradient and the concentration level. The seasonal satellite data reveals however higher semi-labile DOC mainly in the southern MAB during summer than in spring while the model shows the opposite. This suggests that the use of a second phytoplankton group is necessary

to simulate adequately the spring–summer dynamics of regenerated primary production and semi-labile DOC. On Georges Bank, the DOC dynamics show no major accumulation in the surface water during spring (Fig. 5a) in agreement with the observation (Chen et al., 1996).

The simulated (with DOM) and observed (SeaWiFS) monthly mean of surface chlorophyll concentration are compared for the post-bloom period (June 2004), i.e. at a critical moment for the buildup of DOC pool. The high chlorophyll levels agree well on particularly in the inner-shelf and on Georges Bank due to the tidal mixing and permanent nutrient availability. A feature which is partially observed by the satellite sensor in the Georges Bank area but appears in the model and is well documented (Ryan et al., 1999) is the enhancement of surface chlorophyll at the shelf break of the MAB and southern Georges Bank from mid-April to late June. These higher chlorophyll concentrations correspond to the transition period from well-mixed to stratified conditions and is sustained by the upwelled nitrate-rich waters of the geostrophic jet that flows along the shelf break and slope from Georges Bank to Cape Hatteras (Ryan et al., 1999; Fig. 8a). Although the satellite-derived chlorophyll content in the Gulf Stream is higher than in other offshore areas, the model overestimates it (Fig. 6) due to imperfections in the model physics of this highly dynamic area (likely the mixed layer depth).

A novel plot for quantitatively evaluating and displaying the skill of coupled biological–physical models, called the target diagram, has been recently introduced (Jolliff et al., 2009). In these diagrams, bias and centered-pattern RMS are normalized by the standard deviation of the observations and plotted on the x - and y -axes, respectively. Because the sum of the squares of these two

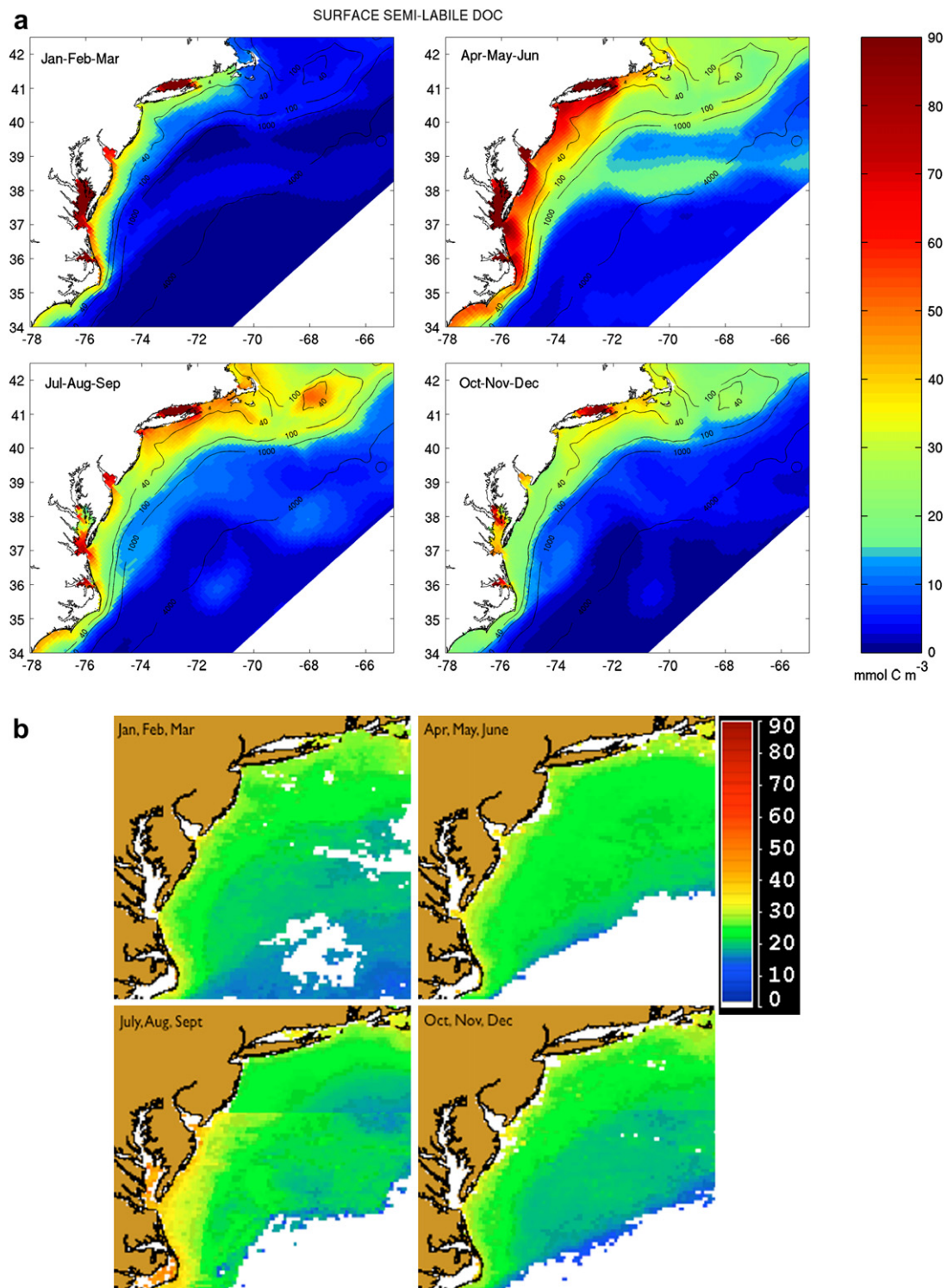


Fig. 5. Seasonal surface concentration of semi-labile DOC (mmol C m^{-3}) for 2004 estimated by the (a) model in the MAB and Georges Bank regions and from (b) the SeaWiFS satellite sensor in the MAB area (see Mannino et al., 2008). Note geographical extension between (a) and (b) are different. Isobaths are in meters.

components of the RMS difference is equal to the square of the total RMS difference, the distance from the origin to each plot symbol represents total RMS error. Although centered-pattern RMS is inherently a positive quantity, in the target diagram the centered-pattern RMS is multiplied by the sign of the difference: standard deviation of observations – standard deviation of model. Thus symbols are plotted with positive x -coordinates if the model

overestimates the data variability and with negative x -coordinates if the model underestimates the data variability. The circle representing total RMS difference = 1.0 (i.e. total RMS equals the standard deviation of the observations) is typically superimposed on these diagrams for reference. By definition, model results falling within this circle reproduce observed quantities better than the mean of those observations.

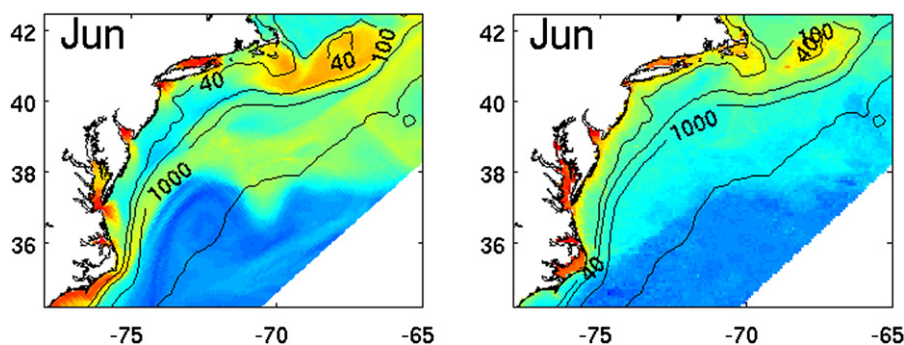


Fig. 6. Surface chlorophyll concentration (mg Chl m^{-3}) simulated by the model (left) and observed by the satellite sensor SeaWiFS using the algorithm OC4V4 for June 2004 in the MAB and Georges Bank regions.

Target diagrams for both model runs (with and without DOM) are presented in Fig. 7, and illustrate the skill of the models in reproducing the satellite monthly mean surface chlorophyll concentrations (2004) for the region encompassing the mid- and outer-shelf and slope of the MAB. Overall the target diagrams

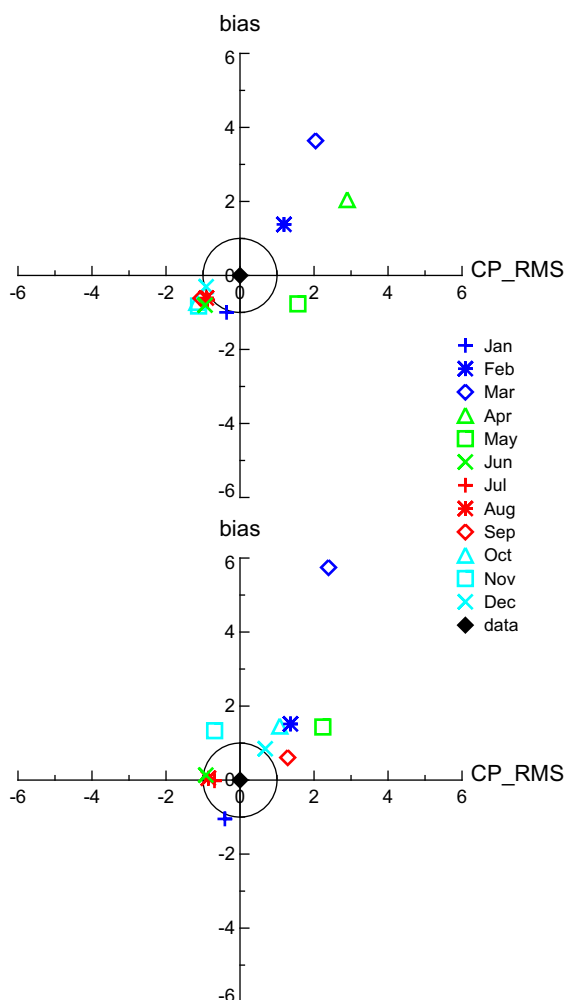


Fig. 7. Target diagrams (representing the total RMS difference, see text for details) of the monthly mean of surface chlorophyll concentration between the model estimate and derived from satellite (SeaWiFS sensor) for the reference run without DOM (upper) and the model run including DOM (lower). The area included in this evaluation comprises the mid- and outer-shelf and the slope of the MAB. Note that a positive bias and centered-pattern RMS correspond to an overestimation compared to the satellite estimate of the model chlorophyll value and spatial variability respectively.

demonstrate that both model simulations produce monthly chlorophyll concentrations comparable to SeaWiFS with March and April as the exceptions (April for the run with DOM has a bias of 6.5, thus just falling out the axes). The reference run generally (except February–April) underestimates the surface chlorophyll content (negative bias), whereas the DOM run more often overestimates surface chlorophyll (except in January, Fig. 7). Both simulations overestimate the spatial variability of surface chlorophyll in February–May (positive centered-pattern RMS). From June to August, both simulations underestimate similarly the observed spatial variability to the same degree. However in these summer months, when the DOM plays an important role in sustaining the phytoplankton production, the model results are negatively biased (underestimation) in the run without DOM whereas the bias is nearly zero for the run with DOM.

The organic carbon production in the MAB and Georges Bank regions (Fig. 8c) range between 100 and 300 $\text{g C m}^{-2} \text{yr}^{-1}$ in general agreement with previously published values (Falkowski et al., 1988 and Berger, 1989: 120–300 $\text{g C m}^{-2} \text{yr}^{-1}$) with little alongshore variability in the central MAB (O'Reilly and Busch, 1984). However, this level of productivity is lower than the approach using mixed satellite and in situ profiles with values of 320 $\text{g C m}^{-2} \text{yr}^{-1}$ on the shelf, 304 $\text{g C m}^{-2} \text{yr}^{-1}$ on the shelf break and 411 $\text{g C m}^{-2} \text{yr}^{-1}$ on the slope of the northern MAB (Mouw and Yoder, 2005). Compared to prior estimates of primary productivity for the Georges Bank region (O'Reilly et al., 1987), the model estimates are too low by approximately 100 $\text{g C m}^{-2} \text{yr}^{-1}$.

The seasonal variability of simulated primary production on Georges Bank (Fig. 3a) from May to September are in agreement with measurements (slightly above 1 $\text{g C m}^{-2} \text{d}^{-1}$, O'Reilly et al., 1987), but the December–March levels of productivity of 0.01–0.10 $\text{g C m}^{-2} \text{d}^{-1}$ in the model are significantly lower than observations (0.2–0.6 $\text{g C m}^{-2} \text{d}^{-1}$). The lack of a low-light sensitive phytoplankton group in the model is believed to be the cause of the winter underestimation of productivity. The percentage of extracellular release (PER) shown on Fig. 3 is in agreement with the measurements of O'Reilly et al. (1987) between 14% in the shallow water (8–23% at station 1) and 21% over the slope of Georges Bank. Daily primary production levels simulated at station 2 (Fig. 3b) are also in agreement with the measurement of the SEEP-I experiment in 1984 with 0.60 $\text{g C m}^{-2} \text{d}^{-1}$ in March and 1.33 $\text{g C m}^{-2} \text{d}^{-1}$ in April (Falkowski et al., 1988). The inner-shelf north and south of the Delaware Bay show a much stronger underestimation of productivity in the model (100 $\text{g C m}^{-2} \text{yr}^{-1}$) than the observation (505 $\text{g C m}^{-2} \text{yr}^{-1}$, O'Reilly et al., 1987). In that particular area, the phytoplankton is nitrogen-limited, and the lack of sediment erosion by waves and POM resuspension is believed to cause this discrepancy. The levels of productivity provided by the model in

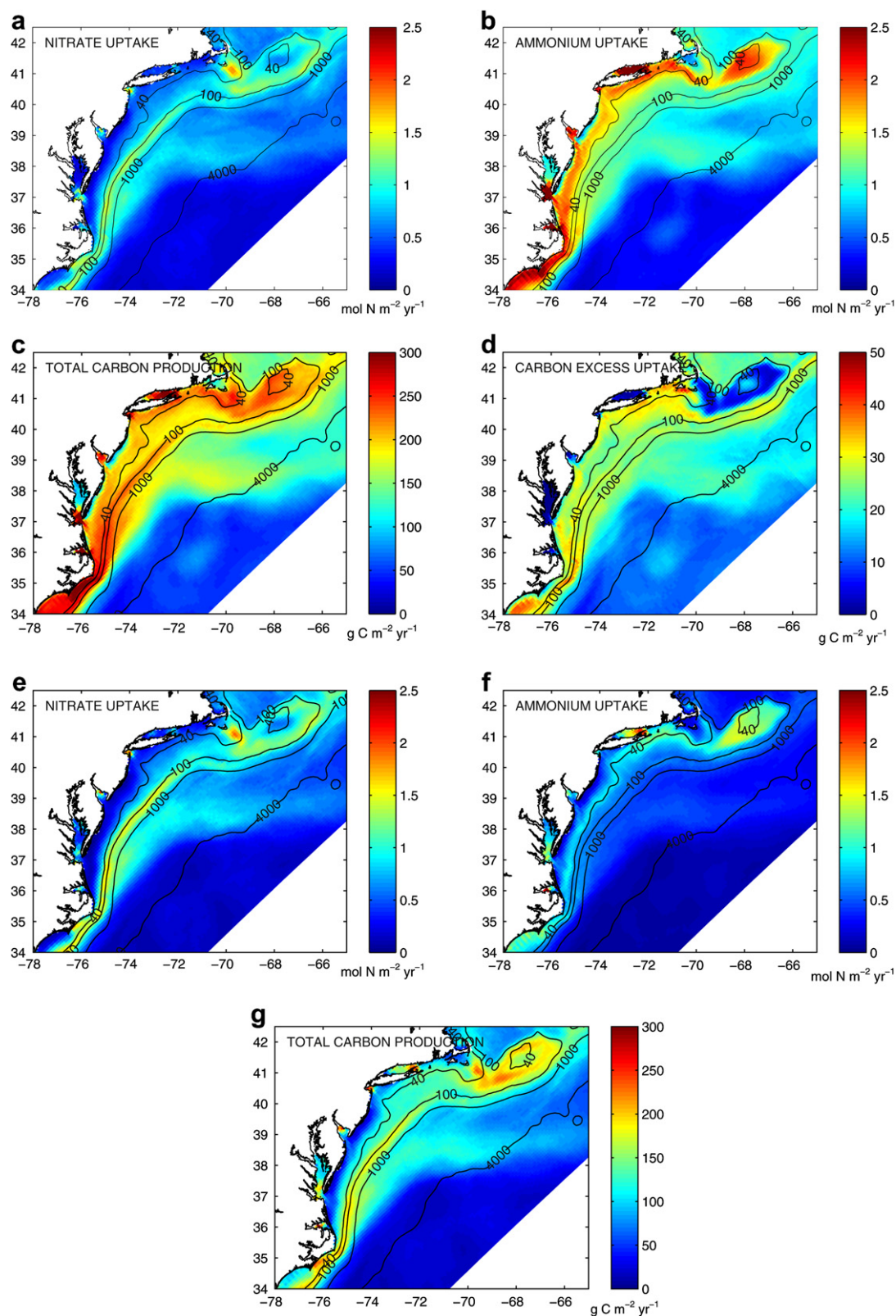


Fig. 8. Comparison of the annual nutrient uptake and carbon production rates for the model run with the DOM module (left panels) and without DOM (right panels): (a) nitrate uptake (new production, $\text{mol N m}^{-2} \text{yr}^{-1}$), (b) ammonium uptake (regenerated production, $\text{mol N m}^{-2} \text{yr}^{-1}$), (c) total carbon primary production ($\text{g C m}^{-2} \text{yr}^{-1}$) and (d) carbon excess uptake ($\text{g C m}^{-2} \text{yr}^{-1}$) estimated by the DOM model for 2004 in the MAB and Georges Bank regions. Panels (e), (f) and (g) are the same model outputs as (a), (b), and (c) for the simulation without the DOM model. In the DOM model, the carbon excess uptake of DIC represents an ‘overflow’ of photosynthesis under nutrient limitation, resulting in DOC production.

the southern MAB shelf between the Chesapeake Bay mouth and Cape Hatteras ($0.5\text{--}1.0\text{ g C m}^{-2}\text{ d}^{-1}$ in March and July) are in the range of field data ($0.5\text{--}1.0\text{ g C m}^{-2}\text{ d}^{-1}$ in March and $0.5\text{--}2.0\text{ g C m}^{-2}\text{ d}^{-1}$ in July, Verity et al., 2002). With the exception of the inner-shelf of the MAB, the productivity is thus well reproduced for the spring–summer–autumn period when most of semi-labile DOC variability occurs.

3.3. Semi-labile DOC export to the open ocean and POC burial

The annual mean horizontal divergence of semi-labile DOC integrated over the water column (Fig. 9a) shows specific areas of production, areas of export (positive values) and import (negative values) for both the shelf and the open ocean. Areas of high primary production are identified as regions of significant export

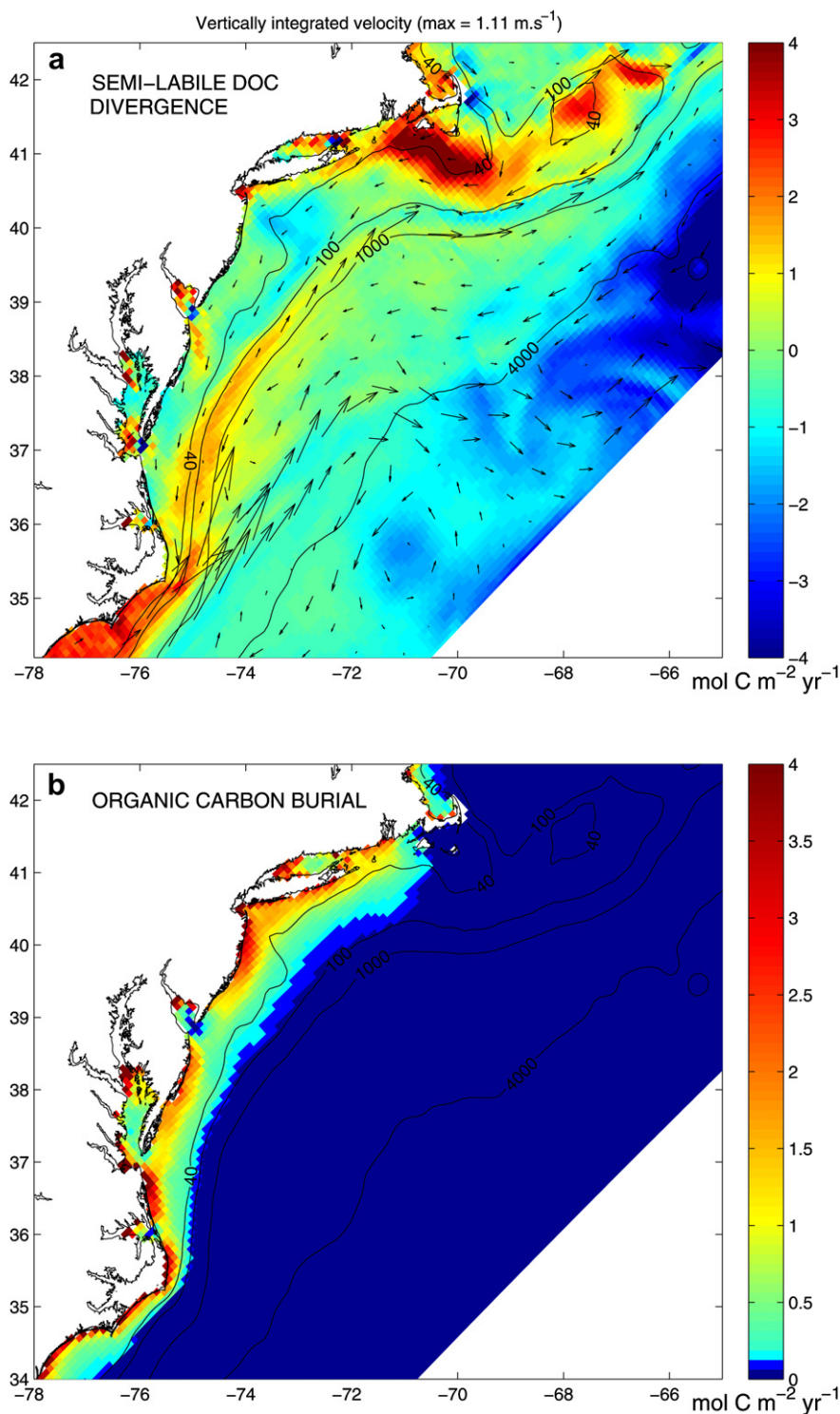


Fig. 9. (a) Net horizontal transport of semi-labile DOC ($\text{mol C m}^{-2}\text{ yr}^{-1}$) estimated by the model for the year 2004 in the MAB and Georges Bank regions: positive values are areas of production and export of semi-labile DOC and negative values are areas of import. (b) Carbon burial ($\text{mol C m}^{-2}\text{ yr}^{-1}$) for the same area and period.

of semi-labile DOC. The DOC release in Georges Bank and the shelf south of Cape Cod is mainly exported to the central MAB shelf. The DOC released on the southern outer-shelf and slope of the MAB and off Cape Hatteras is exported to the adjacent deeper ocean. Both areas of export and import show an annual flux on the order of $1 \text{ mol C m}^{-2} \text{ yr}^{-1}$.

POC deposition at the seabed was fairly well represented by the model. POC deposition rates on the shelf off Delaware Bay and Chesapeake Bay of 2.7 and $2.1 \text{ mol C m}^{-2} \text{ yr}^{-1}$ respectively (Biscaye et al., 1994) are in agreement with the model which ranges from 1.0 to 2.5 and from 1.0 to $4.0 \text{ mol C m}^{-2} \text{ yr}^{-1}$ respectively (results not shown). The model, however, underestimates approximately ten-fold the POC deposition on the slope compared to field measurements (4.6 – $13.1 \text{ mol C m}^{-2} \text{ yr}^{-1}$ off Cape Hatteras and 1 – $2 \text{ mol C m}^{-2} \text{ yr}^{-1}$ on other slope areas of the MAB, Biscaye et al., 1994; Schaff et al., 1992; Thomas et al., 2002). This suggests that the sinking velocity of the large detritus is too low or a third 'very large' detritus pool with sinking velocities of 100 m d^{-1} (Walsh, 1994) is lacking in the model for deep estimates.

Contrary to POC deposition, carbon burial on the shelf is not well documented in the literature. Although the burial is probably slightly underestimated, together with primary production, we believe the model estimate of POC burial (Fig. 9b) is realistic since the POC deposition rate agrees with field measurements and the simulated POC burial on the shelf is globally higher (from 1.5 to $4.1 \text{ mol C m}^{-2} \text{ yr}^{-1}$) than field estimates on the slope (1 – $2 \text{ mol C m}^{-2} \text{ yr}^{-1}$). The maxima in POC burial (Fig. 9b) occur on the inner-shelf south of the dominant simulated rivers and estuaries from 1.5 up to $4 \text{ mol C m}^{-2} \text{ yr}^{-1}$. Except for the region south of Cape Cod and Georges Bank where the tidal-induced bottom friction prevents deposition, the rest of the shelf shows decreasing values of POC burial from inshore to offshore, with a flux of about 0.5 – $1 \text{ mol C m}^{-2} \text{ yr}^{-1}$ along the 40 m isobath. For water depth greater than 100 m in the MAB, the POC is entirely mineralized in the water column. The burial of PON has the same geographical distribution as POC with a C–N ratio of 9.3 (see Appendix).

4. Discussion

4.1. Impacts of the DOM on the ecosystem model

In the simulation without DOM, the POM pools are directly remineralized to DIC and ammonium using the same rates as in Fennel et al. (2006), i.e. 0.03 d^{-1} for small detritus and 0.01 d^{-1} for large detritus. Otherwise, the parameterization is the same for both simulations. The main impact of the introduction of DOM to the model is a large increase in regenerated production (ammonium uptake) from 30% at Georges Bank and shelf break, 50% over the slope and deep ocean, to 250 – 300% in the mid- and inner-shelf of the MAB (Fig. 8b and f). In contrast, the nitrate uptake shows globally the same distribution and level. The total carbon production shows an increase up to $60 \text{ g C m}^{-2} \text{ yr}^{-1}$ in the open ocean and the deeper Georges Bank (between 40 and 100 m , station 1), among which 0 – $20 \text{ g C m}^{-2} \text{ yr}^{-1}$ is linked to the carbon excess uptake. The increase in productivity ranges from 60 to $90 \text{ g C m}^{-2} \text{ yr}^{-1}$ in the outer-shelf and the most of the slope and from 90 to $180 \text{ g C m}^{-2} \text{ yr}^{-1}$ in the inner- and mid-shelf among which 20 – $35 \text{ g C m}^{-2} \text{ yr}^{-1}$ is related to carbon excess uptake. This enhanced production is mainly (65 – 100%) caused by the progressive mineralization of the semi-labile DON in surface waters in summer and autumn (Fig. 4c). The productivity supported by DON during summer and autumn could explain the usual underestimation of models which do not include DON (e.g. Fennel et al., 2006). Only 0 – 35% of this increase depending on the level of nutrient depletion is related to the 'extra' production of

carbohydrates. The constant supply of nutrient by the tidal-induced mixing on Georges Bank reduces the importance of DON as a source of nitrogen in the upper layer as shown by the small difference in primary production between the two simulations (Fig. 3, station 1). The phytoplankton biomass and chlorophyll levels are also dramatically lower without the DOM module, particularly in the MAB shelf and slope (Fig. 7). The target diagrams demonstrate the improvement in estimating surface chlorophyll in summer for the DOM model simulation, but worsened for March and mid-autumn.

4.2. The semi-labile DOM dynamics

The model highlights that the most important contributor to the semi-labile DOC near the surface at station 3 is the phytoplankton exudation. The exudation mainly occurs in the mixed layer during the stationary and decaying phases of the bloom and between the mixed layer depth and the 10% isolume during summer. Note that the carbon excess-based contribution of the exudation in summer takes place in the upper part of this subsurface layer where phytoplankton are nutrient-limited and not light-limited. In contrast, the nutrient-based release takes place in the deeper and light-limited areas. The other important contributor to DOC release is the POC solubilization which occurs in deeper waters. The vertically integrated flux of DOC release by POC solubilization is about three times greater than the release by exudation although it is more equally distributed in the water column. The smallest contributor to DOC release at station 3 is sloppy feeding by zooplankton, which accounts for approximately 1% of the annual release, although it temporarily reaches 10% of the total DOC release at the end of the spring bloom. This simulated rate can reach 50% in highly productive areas such as the Chesapeake Bay mouth during a bloom in agreement with the field estimates (Møller et al., 2003).

The vertically integrated reservoir of semi-labile DOC at station 3 is 1.5 times higher than the carbon detritus pool and twice the carbon standing stock of phytoplankton. At station 1 and 2, the semi-labile DOC pool is twice the POC pool and four times the carbon phytoplankton pool. It represents therefore the largest freshly produced organic pool of carbon in the water column on the mid- and outer-shelf. It can be efficiently exported by horizontal transport (see next section) since this organic carbon is dissolved and slowly mineralized. Model results suggest that a large fraction of the carbon dioxide entering the shelf ocean is stored in semi-labile DOC, while 12 – 14% of the CO_2 flux is buried at stations 2 and 3 (less at station 1 where tidal mixing prevents deposition).

4.3. Carbon export

The annual carbon dioxide air–sea flux simulated by the model is positive (carbon sink) for the studied waters except in the upper part of the Chesapeake Bay where a continuous flow of terrestrial organic materials favors the mineralization and generates a source flux of dissolved CO_2 to the atmosphere. The annual CO_2 flux ranges from 0.5 to $2.0 \text{ mol C m}^{-2} \text{ yr}^{-1}$ in the deep ocean and on the shelf except South of Cape Cod and Georges Bank where values range from 2 to $5 \text{ mol C m}^{-2} \text{ yr}^{-1}$. This is in agreement with the estimation of a net annual uptake of $\sim 1 \text{ mol m}^{-2} \text{ yr}^{-1} \text{ CO}_2$ in the MAB (DeGrandpre et al., 2002). Since the carbon-rich DOM buildup contributes to CO_2 drawdown seasonally (Sambrotto et al., 1993), the results suggest that a large amount of the carbon entering the surface ocean is temporarily stored in the DOC reservoir.

The carbon export of POC from the shelf to the slope has been studied extensively (e.g. Biscaye and Anderson, 1994; Thomas

et al., 2002) and was shown to be particularly important near Cape Hatteras where both the MAB (Mayer et al., 2002) and SAB production (Schaff et al., 1992) contribute to the shelf-slope carbon efflux due to the converging shelf circulation. The comparison presented in Fig. 9 shows that POC is buried in the inner- and mid-shelf of the MAB at rates comparable to the export of seasonally produced DOC from the outer-shelf and slope to the open ocean. In contrast to the southern MAB, the DOC produced at Georges Bank and south of Cape Cod is mostly exported southward to the central MAB shelf between Long Island and Delaware Bay and does not contribute to a net export to the deep ocean.

5. Conclusion

This study describes a twin experiment where a circulation model coupled to a carbon and nitrogen biogeochemical model is tested with and without the major DOM production processes. The test aims at estimating (1) the role of DOM in the coastal ecosystem C and N cycling and (2) the relative importance of the export of freshly produced DOC to the open ocean compared to POC burial on the shelf. In nutrient-depleted and light-replete conditions, the production of carbohydrate by phytoplankton partially decouples the carbon and nitrogen primary productivity. The results show that the introduction of DOM in the model increases primary production by 60–180 g C m⁻² yr⁻¹ in the MAB, of which 65–100% is caused by the ammonium release from DON mineralization in the upper layer and 0–35% is linked to the 'excess' production of carbohydrates. In terms of flux, the annual release of semi-labile DOC by the near-surface phytoplankton exudation can be three times lower than the POC solubilization in the water column. The seasonally produced DOC export from the shelf to the open ocean takes place mostly in the southern outer-shelf and slope of the MAB at a comparable rate to POC burial in the inner- and mid-shelf (~1–2 mol m⁻² yr⁻¹). Subsequent steps in model development will consider the inclusion of the refractory DOC, multiple phytoplankton and zooplankton functional groups, a diagenetic sub-model to simulate remineralization and burial in the sediment, a fast sinking detritus (~100 m d⁻¹) and a higher horizontal resolution in shallow areas. The model parameterization and evaluation will also be improved by using surface DOC and POC concentration derived from satellite remote sensing. These refinements will allow for a more complete estimate of the carbon budget at the scale of the Eastern U.S. continental shelf and provide for a better understanding of the role of DOC in the dynamics of carbon cycling at the land–ocean interface.

Acknowledgments

This work was supported by a NASA postdoctoral associateship arranged by Dr. Paula Bontempi, the NASA Ocean Biology and Biogeochemistry Program Manager, in the frame of the NASA Interdisciplinary Science Project U.S. Eastern Continental Shelf Carbon Budget (USECoS, <http://www.ccpo.odu.edu/Research/US-ECOS/>). We wish to thank John O'Reilly, Cindy Lee, Eileen Hofmann, Ray Najjar and Dale Haidvogel for the constructive discussions and suggestions on the project and Rutgers University, Institute of Marine and Coastal Sciences, for supplying the computer resources. The manuscript benefitted from comments provided by the editor, Ivan Valiela, and an anonymous reviewer. We thank the NASA Ocean Biology Processing Group for processing and distribution of SeaWiFS data.

Appendix

A.1. DOM processes and model description

DOM production by phytoplankton

An overview of the literature highlights two phases of DOC production by phytoplankton. Søndergaard et al. (2000) suggest in their study that exponentially growing communities produce the most labile DOC, whereas declining and nitrogen-deficient communities produce the least labile DOC. During the growth phase, DOM production is linked to biomass and dominated by the exudation of labile-low molecular weight (LMW) organic compounds (Jensen, 1983; Lancelot, 1984; Biddanda and Benner, 1997) with a C–N ratio of ~7 (range 3–11 depending on species [~6.6 for the diatom sp. *Skeletonema*], Biddanda and Benner, 1997). In fact, the exudation was shown to be a passive diffusion across the outer cell membrane that occurs as long as new products of photosynthesis are available (Marañón et al., 2004). During the stationary and decaying phase of the bloom (i.e. under nutrient stress), large quantities of semi-labile, high molecular weight (HMW) DOM with high C–N ratios (10–25 compiling results of Benner et al., 1992) would be released as a result of the exudation of polymeric carbohydrates (Lancelot and Billen, 1985) or due to cell lysis and to 'sloppy' feeding by zooplankton.

Some evidence suggests that the release of carbohydrates by phytoplankton could mainly explain the accumulation of semi-labile DOC after the spring bloom and its progressive remineralization during summer and autumn. Biddanda and Benner (1997) showed that the relative abundance of carbohydrates in phytoplankton DOC increased from 23% during the exponential phase to 80% during the decay phase. Continued maintenance of photosynthetic machinery after nutrient exhaustion was found to be accompanied by excretion of DOM and especially carbohydrates with high C–N ratio (Hellebust, 1965; Norrman et al., 1995). Diatoms can continue to excrete polysaccharides for a considerable time after the halt of cellular protein synthesis (Jensen, 1983). In many offshore systems, a DOC decrease is found to continue after nutrient exhaustion (Sambrotto et al., 1993). The semi-labile DOC release would thus occur mainly in low nutrient conditions and is likely to be associated with phytoplankton primary production. Furthermore, the spring–summer accumulation of DOC would be related to microzooplankton grazing on bacteria coupled to low bacterial growth rates, which would reduce DOC remineralization and allow DOC accumulation (Thingstad et al., 1997).

Two models of extracellular DOM release have been proposed: the overflow model (Fogg, 1966, 1983; Williams, 1990; Nagata, 2000) and the passive diffusion model (Fogg, 1966; Bjørnsen, 1988). Even if these models were opposed in conflicting reports, it is likely that they are not mutually exclusive and that both models are correct given the right environmental conditions and plankton community structure (Carlson, 2002). Carlson suggests that the extracellular release of labile-LMW-DOM model is likely to be a passive diffusion process linked to biomass. During the stationary and decay phases, the overflow model is likely to represent an active release of semi-labile-HMW-DOM linked to primary production and enhanced in a nutrient-depleted environment. Because primary production is traditionally expressed in models as a function of biomass, both terms of exudation (labile) and excretion (semi-labile) of DOM are dependent on primary production in the present model (and in most other modeling studies, e.g. Anderson and Williams, 1998).

Exudation of labile DON and nutrient-based labile DOC

The excretion as amino acids was estimated to be approximately 3% of the assimilated nitrate (Admiraal et al., 1986). The rate chosen

for the labile DON exudation (and instantaneous mineralization in the model) is set to $\omega_N = 3\%$ of phytoplankton nitrogen production. The labile DOC leakage is also expressed as a function of primary production with the same rate ($\omega_C = 3\%$) to ensure a constant Redfield ratio for labile DOM and phytoplankton.

Semi-labile DON exudation by phytoplankton

The average release of DON was found to be of 25–41% of the inorganic nitrogen uptake in offshore oceanic (25%), coastal (27%) and estuarine (41%) environments with turnover times of 10 ± 1 , 18 ± 14 , and 4 days respectively (Bronk et al., 1994). Since the labile fraction of DON production is estimated to be a few percent of DIN uptake (3%, see above), the semi-labile DON total release in the coastal ocean is estimated at 24% of nitrogen-based primary production with a decreasing value offshore. Varela et al. (2003) provided some evidence that DON production is dominated by grazing processes rather than by direct phytoplankton excretion. Large DON losses (>50% of nitrogen uptake) were attributed to intense grazing and sloppy feeding for several marine ecosystems (Bronk and Ward, 2000). The maximum of DON release was found to occur when small, presumably heterotrophic, flagellates dominated the biomass and not the primary production (Varela et al., 2003), i.e. sloppy feeding by flagellates could significantly increase the DON release. In summary, sloppy feeding might dominate the DON release during a short period of intense grazing, but phytoplankton exudation and detritus solubilization dominates otherwise. It is estimated that the DON released by exudation follows a Redfield ratio of the nutrient-based DOC exudation that is set to 4% of primary production (basal value of DOC exudation by healthy phytoplankton, see next subsection). The rate of semi-labile DON exudation by phytoplankton (ε_N) is set to 4% of nitrogen-based primary production. Following the above assumption that semi-labile DON release should be 24% of primary production in most of the continental shelf, the sloppy feeding should account for 3–15% (low and high grazing) and PON solubilization for 17–5% depending on grazing.

Nutrient and carbon excess-based semi-labile DOC exudation by phytoplankton

In their mesocosm experiment, Norrman et al. (1995) observed that 23% of total new production accumulated as DOC, which was found to increase due to a combination of excretion and cell lysis. A large range of values of DOC production as a fraction of primary production can be found in the literature (5–30%, Biddanda and Benner, 1997; Norrman et al., 1995; Vlahos et al., 2002), however excretion from natural healthy phytoplankton was found to be lower (4–16%) than at the end of a diatom bloom (17–38%, Hellebust, 1965).

Two terms describe the semi-labile DOC exudation by phytoplankton in the model: a nutrient-based and carbon excess-based release. The nutrient-based release reflects the healthy phytoplankton exudation of semi-labile DOC and follows the semi-labile DON exudation with the Redfield ratio. The carbon excess-based release represents the carbohydrate over-production by nutrient-stressed cells. The carbon excess uptake is seen as an 'overflow' of photosynthesis under nutrient limitation. It is formulated as the difference between the nutrient-saturated (light-limited) and nutrient-limited (light-limited) primary production and is directed to the semi-labile DOC (Anderson and Williams, 1998; Ianson and Allen, 2002, see Fig. A.1 with the details of the terms in Table 1). The carbon excess uptake ($U_{exc.C}$) is thus expressed:

$$U_{exc.C} = \gamma CN_P (PP_L - PP_L L_N)$$

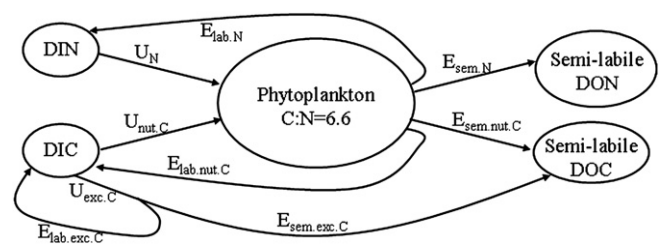


Fig. A.1. Diagram of the fluxes involved in the uptake and exudation of nitrogen and carbon. See Table 1 for details.

where PP_L is the nutrient-based primary production limited by light, L_N is the nutrient limitation, CN_P is the C–N ratio for phytoplankton and γ the parameter of carbon excess-based DOC excretion by phytoplankton. A fraction (σ_C) of the carbon excess uptake is directed to the semi-labile DOC pool and represents the exudation of carbon excess-based DOC release. This fraction is set to $\sigma_C = 0.45$ (Biddanda and Benner, 1997 found ~35%). The labile DOC originating from carbon excess uptake represents a slightly higher fraction ($1 - \sigma_C$) and is directed back to DIC.

The total excretion is commonly expressed as a fraction of the total carbon fixed by phytoplankton, the percentage extracellular release (PER). In the present setting, the PER follows:

$$\begin{aligned} PER &= 100 \left(\frac{E_{lab.nut.C} + E_{sem.nut.C} + E_{lab.exc.C} + E_{sem.exc.C}}{U_{nut.C} + U_{exc.C}} \right) \\ &= 100 \left(1 - \frac{1 - \omega_N - \varepsilon_N}{1 + \gamma \left(\frac{1}{L_N} - 1 \right)} \right) \end{aligned}$$

The PER for diatoms was estimated to be between 10% and about 55% (Baines and Pace, 1991; Obernosterer and Herndl, 1995) with an increase between the exponential and the stationary phase of the bloom. Higher PER values (70–80%) were observed in eutrophic water for *Phaeocystis pouchetii* (Lancelot, 1983). The analytical formulation of the PER in our model shows that the mean PER is lower than 65% for L_N below 0.5 (nutrient limiting condition) when γ is set to 0.20. We thus chose $\gamma = 0.20$ for the simulations. For comparison, Anderson and Williams (1998) adjusted γ to 0.26 to achieve the desired spring DOC concentration and obtained PER values between 10% and 60% for station E1 in the English Channel.

Table 1

Summary of the terms involved in the uptake and exudation of nitrogen and carbon by phytoplankton. PP_L is the nutrient-based primary production limited by light, L_N is the nutrient limitation, CN_P is the C–N ratio for phytoplankton and γ the parameter of carbon excess-based dissolved organic carbon (DOC) excretion by phytoplankton (see Table A1 for the definition of other parameters).

Expression	Description
$U_N = PP_L L_N$	Nitrogen-based primary production or uptake of nitrogen
$U_{nut.C} = CN_P U_N$	Nutrient-based primary production in carbon
$E_{lab.N} = \omega_N U_N$	Exudation of labile DON (directed to ammonium)
$E_{lab.nut.C} = CN_P \omega_N U_N$	Exudation of labile DOC (directed to DIC)
$E_{sem.N} = \varepsilon_N U_N$	Exudation of semi-labile DON
$E_{sem.nut.C} = CN_P E_{sem.N}$	Nutrient-based exudation of semi-labile DOC
$U_{exc.C} = CN_P \gamma PP_L (1 - L_N)$	Carbon excess uptake by nutrient-stressed phytoplankton
$E_{lab.exc.C} = (1 - \sigma_C) U_{exc.C}$	Carbon excess-based exudation of labile DOC
$E_{sem.exc.C} = \sigma_C U_{exc.C}$	Carbon excess-based exudation of semi-labile DOC

DOC release by 'Sloppy' feeding

Measurements from the literature suggest a high DOC release when the prey is large relative to the copepod and low DOC release when the prey is small relative to the copepod (Møller, 2005). During a diatom bloom, sloppy feeding was, by far, the most important contributor to the DOC production by *Calanus* spp., and 49% of the carbon removed from suspension by the copepods was returned to the water column as DOC (Møller et al., 2003). A significant relationship between the DOC production through sloppy feeding by zooplankton and the copepod-to-prey size ratio was found (Møller, 2005). Q defines the fraction of prey carbon removed from suspension and lost as DOC for copepod:prey size ratio below 55: $Q = 0.714 - 0.013$ ($ESD_{\text{copepod}}/ESD_{\text{prey}}$) where ESD is the equivalent spherical diameter.

According to Møller et al. (2003), when copepods graze large diatom cells in spring the copepod:prey size ratio can reach a minimum of 10 and Q values may reach 71%. For an increasing size ratio, i.e. when copepods graze on smaller prey during summer, Q decreases linearly down to $Q = 0.1\%$ for a size ratio of 55 (or more). In agreement, Møller (2005) illustrates that when the prey is large relative to the copepod, i.e. during a bloom of large cells, copepods lose significant amounts of dissolved material. In contrast, the link between copepod feeding and energy flow to higher trophic levels is tighter when the prey is small, i.e. during oligotrophic periods when small cells dominate the phytoplankton prey. The fraction of DOC released by sloppy feeding is likely to reach its maximum during the spring bloom (large diatoms) and minimum in summer when smaller cells are grazed. Since a high grazing level is a good proxy of high biomass of large cells (diatom spring bloom), a linear relationship is used to enhance the fraction of DOC release by sloppy feeding at high grazing levels:

$$Q_{\text{DOC}} = 0.71 \left(\frac{g}{g_{\text{max}}} \right) = 0.71 \left(\frac{\text{Phy}^2}{k_p + \text{Phy}^2} \right)$$

where g is the grazing, g_{max} is the maximum grazing rate, $g = g_{\text{max}}(\text{Phy}^2/(k_p + \text{Phy}^2))$ (Fennel et al., 2006) and k_p is the half-saturation constant of phytoplankton ingestion. The maximum fraction of DOC release of 71% is thus encountered when the grazing intensity is maximum, i.e. at the highest levels of phytoplankton biomass.

The fraction of semi-labile DOC (to total DOC) in the phytoplankton cell is estimated using the work of Biddanda and Benner (1997). They estimated that dissolved carbohydrates represent the major part of cell DOC during the stationary phase of the bloom. They measured a fairly stable fraction of dissolved polysaccharide carbohydrate (between 78 and 94% with a mean of 85%) compared to dissolved monosaccharide carbohydrate between the exponential growth and the stationary phase. However, dissolved polysaccharides (particularly fresh material) can be rather labile (Mannino, 2000; Mannino and Harvey, 2000), therefore the fraction of semi-labile DOC compared to labile DOC is set to $\delta_c = 55\%$. Although the cell-content of DOC is constant in the model, Biddanda and Benner (1997) measured an increase of dissolved carbohydrates from 23 to 80% of cell DOC for four phytoplankton groups (*Synechococcus*, *Phaeocystis*, *Emiliana* and *Skeletonema*) from the growth to the decay phase. The sloppy feeding related terms for carbon are therefore the following:

$$\begin{aligned} \text{Assimilation of organic carbon by zooplankton} &= \text{CN}_p \beta g \\ \text{Semi-labile DOC release by sloppy feeding} &= \text{CN}_p (1 - \beta) Q_{\text{DOC}} \delta_c g \end{aligned}$$

$$\begin{aligned} \text{Labile DOC (towards DIC) release by sloppy feeding} &= \text{CN}_p (1 - \beta) \\ &Q_{\text{DOC}} (1 - \delta_c) g \\ \text{Fecal pellets production (to large detritus)} &= \text{CN}_p (1 - \beta) \\ &(1 - Q_{\text{DOC}}) g \end{aligned}$$

where β is the zooplankton assimilation rate.

DON release by 'sloppy' feeding

Hasegawa et al. (2001) found that 9–75% of ingested nitrogen is assimilated in zooplankton biomass depending on food concentration. Therefore, from 25 to 91% of grazed nitrogen is released as PON, DON or ammonium for low and high food concentrations respectively through the processes of sloppy feeding, excretion and egestion of fecal pellets. Zooplankton excretion rates in the original model (Fennel et al., 2006) included the assimilation-related excretion ($I_E = 0.1 \text{ d}^{-1}$ if grazing is maximum) and the basal metabolism related excretion ($I_{\text{BM}} = 0.1 \text{ d}^{-1}$). The rate of fecal pellet production was set to 25% and the assimilation efficiency to 75%. Therefore, in order to compare with the values of Hasegawa et al. (2001), the fraction of nitrogen released per day in the model by excretion (assuming zooplankton ingests 60% of its weight of prey per day¹) and egestion of fecal pellets was $0.1 \times 0.75 + 0.1 \times 0.6 + 0.25 = 0.385$. This value can decrease to 28.5% if the zooplankton stops grazing. Therefore the model absolute assimilation efficiency ranged from 61.5% for high food condition to 71.5% under low food condition, which is a low range for DON release compared to Hasegawa et al. (2001) (9–75% assimilation). Adding the process of sloppy feeding has the effect of decreasing the absolute assimilation efficiency for high food condition, with a maximum contribution of about 50% of the nitrogen grazed. The assimilation efficiency in the model was constant and linked to fecal pellet production ($\beta = 0.75$). Compared to the original model, β is grazing-dependant taking into account the loss of DON by sloppy feeding. In the current model, the 'absolute' assimilation efficiency (which includes the excretion rates, $\beta - I_E \beta g / g_{\text{max}} - I_{\text{BM}}$) varies between 10 and 75% as a function of the grazing intensity (Hasegawa et al., 2001), which leads to:

$$\beta = \frac{[0.75 + I_{\text{BM}} - 0.65 \frac{g}{g_{\text{max}}}]}{[1 - I_E \frac{g}{g_{\text{max}}}]}$$

where β is the grazing-based assimilation efficiency (excluding the excretion rates). The assimilation efficiency defined here does not include the excretion rates and varies between $\beta = 0.22$ for $g = g_{\text{max}}$ and $\beta = 0.85$ for $g = 0$. The fraction of semi-labile DON to total DON is assumed to be low (the opposite for DOC) and is set to $\delta_N = 30\%$. Q_{DON} being the fraction of total DON to (DON + PON) within the phytoplankton cell, a fraction $(1 - Q_{\text{DON}})$ of the remaining non-assimilated material $(1 - \beta)$ is allocated to the fecal pellets and the complementary fraction (Q_{DON}) lost by sloppy feeding to the DON. Seventy percent $(1 - \delta_N)$ of this last fraction is labile and 30% ($=\delta_N$) is the semi-labile DON.

In summary, the grazing term for nitrogen is divided as following:

$$\begin{aligned} \text{Nitrogen assimilation for zooplankton} &= \beta g \\ \text{Semi-labile DON release by sloppy feeding} &= (1 - \beta) Q_{\text{DON}} \delta_N g \\ \text{Labile DON release by sloppy feeding} &= (1 - \beta) Q_{\text{DON}} (1 - \delta_N) g \\ \text{Fecal pellets production (to large detritus)} &= (1 - \beta) (1 - Q_{\text{DON}}) g \end{aligned}$$

¹ The maximum grazing rate is 0.6 d^{-1} .

Table 2
Release of dissolved combined amino acids (DCAA) flux from aggregates, carbon content of aggregates, fraction of nitrogen in released DCAA estimated by Smith et al. (1992), and DON release rates deduced from these data.

Aggregate type (April 1990)	DCAA release ($\mu\text{g agg}^{-1} \text{d}^{-1}$) (1)	Carbon content ($\mu\text{g C agg}^{-1}$) (2)	Nitrogen fraction in released DCAA (non-dimensional) (3)	DON release rate ($\text{gN}_{\text{DCAA}} \text{gN}_{\text{agg}}^{-1} \text{d}^{-1}$) assuming POC:PON = 5 (1) \times 5.0 \times (3)/(2)
Larvacean house	0.936	3.5	23.3/155.2 = 0.150	0.200
Diatom floc	0.527	3.5	2.4/15.4 = 0.156	0.117
Larvacean house	0.478	3.2	8.0/53.6 = 0.149	0.118
Larvacean house	0.365	4.5	0.5/3.1 = 0.161	0.066

The C–N ratio of semi-labile DOM produced by sloppy feeding in the model, deduced analytically using the terms defined above, has the constant value of 12.1 ($\text{CN}_{\text{p}\delta\text{C}/\delta\text{N}}$) using the current parameter set (see Appendix).

Solubilization of carbon and nitrogen detritus

Smith et al. (1992) showed that bacteria attached to aggregates can express high levels of hydrolytic ectoenzymes which results in the release of DOM. They suggest a preferential solubilization of nitrogen detritus over carbon detritus in agreement with the observed increase in C–N and C–P ratios of sedimenting material with depth. In the experiments, the aggregates released mainly dissolved combined amino acids (DCAA). Solubilization was uncoupled from bacterial uptake, with 50–98% of the DCAA released escaping rapid utilization from attached bacteria. From the data estimated (Smith et al., 1992; Table 2), DON release rates from aggregates are calculated assuming a C–N ratio for POM of ~ 5 (Harvey et al., 1995). The solubilization rates for DON range from 0.066 to 0.200 d^{-1} with a mean of 0.12 d^{-1} . The solubilization rate of the large and small carbon detritus is set to $S_{\text{SDetC}} = S_{\text{LDetC}} = 0.08 \text{d}^{-1}$. The higher rate chosen for the nitrogen detritus solubilization is $S_{\text{LDetN}} = S_{\text{SDetN}} = 0.11 \text{d}^{-1}$ consistent with the carbon detritus specific respiration rate on diatom aggregates of $0.083 \pm 0.034 \text{d}^{-1}$ (Ploug and Grossart, 2000). The fractions of semi-labile DON and DOC cell-contents (δ_{N} and δ_{C}) described above are used to quantify the release of semi-labile DOM by solubilization. The labile DOM generated by solubilization (directed to the ammonium and DIC pools) uses the complementary fractions ($1 - \delta_{\text{N}}$) and ($1 - \delta_{\text{C}}$).

Mineralization of semi-labile DOC and DON

Since the photo-oxidation process is likely to impact refractory DOC, it is not included in the model. Hopkinson et al. (2002) estimated rates for DOC and DON mineralization by bacteria at 19–20 °C in the MAB. The mean DON degradation rate measured (see Table 4 in Hopkinson et al., 2002) with half-life values comprised between 4 days (0.173 d^{-1}) and 365 days (0.0019 d^{-1}) is $0.073 \pm 0.043 \text{d}^{-1}$ with a corresponding value for DOC of $0.055 \pm 0.057 \text{d}^{-1}$. In a recent six-month degradation experiment at 19–20 °C with DOM collected in the MAB, rates of DOC mineralization are between 0.015 d^{-1} and 0.043 d^{-1} (Russ and Mannino, pers. comm.). The values proposed here are 0.029 d^{-1} ($t_{1/2} = 24 \text{d}$) for the semi-labile DOC and 0.060 d^{-1} ($t_{1/2} = 12 \text{d}$) for the semi-labile DON at 19–20 °C. Since temperature dependence is likely to occur with a $Q_{10} = 2$ (Pomeroy et al., 1991), the degradation rate has the following formulation:

$$\text{Mineralization rate } [d^{-1}] = a_0 e^{0.07T}$$

where $a_0 = a_{\text{C0}} = 0.00767 \text{d}^{-1}$ for carbon, $a_0 = a_{\text{N0}} = 0.0153 \text{d}^{-1}$ for nitrogen semi-labile DOM and T is the temperature in °C. Consequently for the semi-labile DOC, the degradation rate ranges between 0.0088 d^{-1} at 2 °C and 0.0545 d^{-1} at 28 °C and between 0.0176 d^{-1} at 2 °C and 0.1086 d^{-1} at 28 °C for the semi-labile DON. Although bacteria are involved in DOM degradation, bacteria are

not explicitly included in the model to avoid the multiplicity of parameters that cannot be calibrated using our dataset. However, bacterial processes such as organic matter mineralization and solubilization of POM are included in the model with a Q_{10} temperature formulation.

A.2. Other modifications to the model of Fennel et al. (2006)

An additional light attenuation coefficient to account for colored dissolved organic matter (CDOM) was added to the water and chlorophyll attenuation in response to an overestimated euphotic depth simulated by the model in the MAB compared to observations. The light attenuation formulation for CDOM absorption correlated to salinity was implemented in agreement with the combined CDOM plus detritus absorption measurements at 443 nm ($a_{\text{CDM}(443)}$, Magnuson et al., 2004) in estuaries (Chesapeake Bay: $0.368 \pm 0.076 \text{m}^{-1}$ in the mid-Bay for a salinity of 12.9 ± 3.2 , $0.284 \pm 0.090 \text{m}^{-1}$ in the lower Bay for a salinity of 20.8 ± 4.9), on the shelf ($0.168 \pm 0.057 \text{m}^{-1}$ in the inshore MAB and $0.070 \pm 0.035 \text{m}^{-1}$ in the offshore MAB) and in oligotrophic waters (0.010 d^{-1} at the BATS station). The formulation used is (with salinity in Practical Salinity Units):

$$K_{\text{CDOM}} = 0.5329 - 0.02669 \times \text{salinity} + 0.0003395 \times (\text{salinity})^2$$

It is slightly lower ($\sim 0.1 \text{m}^{-1}$ for salinity lower than 30) than the observed $a_{\text{CDM}(443)}$ to account for a lower absorption of the PAR in the entire visible spectrum than in the blue (443 nm).

In the present model version, the zooplankton products (dead zooplankton and fecal pellets) and the aggregates of dead phytoplankton cells with small detritus are directed to the large detritus compartments instead of the slow-sinking small detritus compartments in Fennel et al. (2006). As a result in the water column, the small detritus compartments (SDetN and SDetC) are only fed by the dead, non-aggregated, phytoplankton cells and the large detritus compartments (LDetN and LDetC) include the aggregates of dead phytoplankton cells with the small detritus and the zooplankton products.

In order to explore the high POM burial of the U.S. northeastern continental shelf (Thomas et al., 2002) and to compare it with the horizontal export of DOM to the open ocean, a parameterization of POM resuspension and burial was added to the model's bottom boundary formulation. The resuspension rate of the POM flux reaching the seabed is a function of the bottom friction velocity. The resuspended fraction of POM is thus largely dependent on the local near bottom current velocity that is driven by the general circulation and tides on the continental shelf and by wind events in shallow waters. The remaining fraction of PON and POC accumulates and is buried in the sediment assuming that the burial efficiency of the particulate organic carbon is proportional to the vertical flux of POC reaching the seabed (Henrichs and Reeburgh, 1987). The POM resuspension and burial processes are fully described in the Appendix section A.4.

A.3. Parameter set

See Tables A1, A2 and A3.

Table A1
DOM specific parameters.

Symbol	Value or range and unit	Parameter or formulation
ω_N	0.03 [non-dimensional] of primary production (N)	Labile DON exudation rate
ω_C	0.03 [non-dimensional] of primary production (C)	Nutrient-based labile DOC exudation rate
ϵ_N	0.04 [non-dimensional] of N primary production	Exudation rate of phytoplankton semi-labile DON
γ	0.20 [non-dimensional]	Parameter of carbon excess-based DOC exudation
σ_C	0.45 [non-dimensional]	Fraction of semi-labile DOC produced by the carbon excess-based exudation
δ_N	0.30 [non-dimensional]	Fraction of semi-labile DON to total DON within the phytoplankton cell
δ_C	0.55 [non-dimensional]	Fraction of semi-labile DOC to total DOC within the phytoplankton cell
Q_{DON}	0.0–0.71 [non-dimensional]: function of the ratio grazing: maximum grazing (g/g_{max})	Fraction of total DON to (DON + PON) within the phytoplankton cell
Q_{DOC}	0.0–0.71 [non-dimensional]: function of the ratio grazing: maximum grazing (g/g_{max})	Fraction of total DOC to (DOC + POC) within the phytoplankton cell
a_{NO}	0.01530 d^{-1}	Remineralization rate of semi-labile DON at 0 °C ($a_{NT} = a_{NO}e^{0.07T}$, with T in °C)
a_{CO}	0.00767 d^{-1}	Remineralization rate of semi-labile DOC at 0 °C ($a_{CT} = a_{CO}e^{0.07T}$, with T in °C)
S_{SDetN}	0.11 d^{-1}	Bacterial solubilization rate of small N detritus
S_{LDetN}	0.11 d^{-1}	Bacterial solubilization rate of large N detritus
S_{SDetC}	0.08 d^{-1}	Bacterial solubilization rate of small C detritus
S_{LDetC}	0.08 d^{-1}	Bacterial solubilization rate of large C detritus

Table A2
Modified parameterization from Fennel et al. (2006).

Symbol	New value or range, and Unit	Former value	Parameter
α^a	0.020 ($W m^{-2}$) $^{-1} d^{-1}$	0.025 ($W m^{-2}$) $^{-1} d^{-1}$	Initial slope of the $P-I$ curve
μ_{max}^a	1.6 d^{-1}	0.59×1.066^T (T is the temperature in °C, Eppley, 1972)	Maximum growth rate of phytoplankton
CN_2^b	5.0 [non-dimensional]	6.625	Zooplankton C–N ratio
β^b	0.22–0.85 for $g/g_{max} = [1.0–0.0]$ [non-dimensional]	0.75	Zooplankton assimilation efficiency
w_s^c	1.0 $m d^{-1}$	0.1 $m d^{-1}$	Small detritus sinking velocity
w_L^c	10.0 $m d^{-1}$	1.0 $m d^{-1}$	Large detritus sinking velocity

^a The temperature-dependent formulation of Eppley (1972) was shown to underestimate primary production (Brush et al., 2002). Even if a temperature dependency most probably exists in relation to the cell metabolism, the light intensity is the prior control factor. The use of a temperature-dependent formulation led to a latitudinal variation and underestimation (low temperature below the thermocline) of primary production. For a better analysis of the results, the temperature dependency of the maximum growth rate was totally removed.

^b See text for details.

^c Since the dead phytoplankton cells on one hand, and the zooplankton corpses and fecal pellets on the other hand sink with distinct velocities due to their particles size difference, the zooplankton products are flowed to the large particle pool which sinks faster instead of the small particle pool. The aggregation process thus concerns only the phytoplankton living and dead cells. The sinking velocities proposed for such a configuration are 1 $m d^{-1}$ for the small detritus pool (dead phytoplankton cells) and 10 $m d^{-1}$ for the large detritus pool (zooplankton particles and phytoplankton aggregates).

Table A3
Common parameterization with Fennel et al. (2006).

Symbol	Value and unit	Parameter
k_{NO_3}	0.5 $mmol N m^{-3}$	Half-saturation constant for nitrate uptake
k_{NH_4}	0.5 $mmol N m^{-3}$	Half-saturation constant for ammonium uptake
CN_p	6.625 [non-dimensional]	Phytoplankton C–N ratio
g_{max}	0.6 d^{-1}	Maximum grazing rate
K_{phy}	2.0 ($mmol N m^{-3}$) 2	Half-saturation constant for grazing
m_p	0.15 d^{-1}	Phytoplankton mortality
τ	0.005 ($mmol N m^{-3}$) $^{-1} d^{-1}$	Aggregation parameter
θ_{max}	0.053 $mg Chla mg C^{-1}$	Maximum chlorophyll to phytoplankton ratio
l_{BM}	0.1 d^{-1}	Excretion rate due to basal metabolism
l_E	0.1 d^{-1}	Maximum rate of assimilation-related excretion
m_z	0.025 ($mmol N m^{-3}$) $^{-1} d^{-1}$	Zooplankton mortality
w_{phy}	0.1 $m d^{-1}$	Phytoplankton sinking velocity

A.4. Equations of the state variables

Semi-labile DON and DOC

The time rate of change of the semi-labile DON and DOC are:

$$\partial DON/\partial t = \text{Phytoplankton exudation} + \text{Sloppy feeding} + \text{Solubilization small and large N detritus (semi-labile fraction)} - \text{Remineralization semi-labile DON}$$

$$\frac{\partial DON}{\partial t} = \epsilon_N \mu \text{Phy} + (1 - \beta) Q_{DON} \delta_{NG} \text{Zoo} + \dots + \delta_N (S_{SDetN} S_{DetN} + S_{LDetN} L_{DetN}) - a_{NO} e^{0.07T} \text{DON}$$

where μ is the phytoplankton growth rate.

$$\partial DOC/\partial t = \text{Phytoplankton exudation (nutrient-based and carbon excess-based)} + \text{Sloppy feeding} + \text{Solubilization small and large C detritus (semi-labile fraction)} - \text{Remineralization semi-labile DOC}$$

$$\frac{\partial DOC}{\partial t} = CN_p (\epsilon_N \mu \text{Phy} + \sigma_C \gamma [\mu_{max} L_L (1 - L_N)] \text{Phy} + (1 - \beta) Q_{DOC} \delta_{CG} \text{Zoo}) + \dots + \delta_N (S_{SDetN} S_{DetC} + S_{LDetN} L_{DetC}) - a_{CO} e^{0.07T} \text{DOC}$$

where L_L and L_N are the non-dimensional terms that determine light and nutrient limitation, and μ_{max} the maximum phytoplankton growth rate ($\mu = \mu_{max} L_L L_N$).

Phytoplankton

Two sink terms are added in the phytoplankton time rate of change: the exudation terms of semi-labile and labile DON towards DON and ammonium respectively.

- $\partial\text{Phy}/\partial t =$ Phytoplankton growth
- Exudation of semi-labile DON
 - Exudation of labile DON (to NH_4)
 - Grazing
 - Phytoplankton mortality
 - Aggregation with small N detritus
 - Sinking of living cells

$$\frac{\partial\text{Phy}}{\partial t} = \mu\text{Phy}(1 - \varepsilon_N - \omega_N) - g\text{Zoo} - m_p\text{Phy} - \tau(\text{SDet} + \text{Phy})\text{Phy} - w_p \frac{\partial\text{Phy}}{\partial z}$$

where m_p is the phytoplankton mortality rate, τ the aggregation parameter of the small detritus and Phy (towards the large detritus pool) and w_p is the sinking velocity of living phytoplankton cells.

Phy is expressed in nitrogen unit using the constant C–N ratio (CN_p) for accessing carbon units and therefore no equation is required for Phy expressed in carbon. A fraction (σ_C) of the carbon excess uptake represents the semi-labile DOC exudation by phytoplankton and is directed towards the semi-labile DOC.

Chlorophyll

The chlorophyll equation is modified accordingly to the changes of the phytoplankton equation:

- $\partial\text{Chl}/\partial t =$ Chlorophyll production
- Loss by exudation of semi-labile DON
 - Loss by exudation of labile DON (to NH_4)
 - Loss by grazing
 - Loss by phytoplankton mortality
 - Loss by aggregation with small N detritus
 - Loss by sinking of living cells

$$\frac{\partial\text{Chl}}{\partial t} = \rho_{\text{chl}}\mu\text{Chl}(1 - \varepsilon_N - \omega_N) - g\text{Zoo} \frac{\text{Chl}}{\text{Phy}} - m_p\text{Chl} - \tau(\text{SDetN} + \text{Phy})\text{Chl} - w_p \frac{\partial\text{Chl}}{\partial z}$$

where ρ_{chl} is the fraction of phytoplankton growth devoted to the chlorophyll synthesis (Geider et al., 1997):

$$\rho_{\text{chl}} = \theta_{\text{max}}\mu\text{Phy}/\alpha I\text{Chl}$$

where θ_{max} is the maximum ratio of chlorophyll to phytoplankton biomass, α is the initial slope of the phytoplankton growth curve relative to light and I the photosynthetically available radiation.

Zooplankton

The zooplankton, like the phytoplankton, is only expressed in nitrogen units:

- $\partial\text{Zoo}/\partial t =$ Fraction of grazing assimilated
- Excretion (basal metabolism and grazing dependent)
 - Mortality

$$\frac{\partial\text{Zoo}}{\partial t} = g\beta\text{Zoo} - \left(l_{\text{BM}} + l_{\text{E}} \beta \frac{g}{g_{\text{max}}} \right) \text{Zoo} - m_z\text{Zoo}^2$$

The remaining term $[(1 - \beta)g\text{Zoo}]$ is divided between the production of semi-labile and labile DON by sloppy feeding (towards semi-labile DON and DIC respectively) and the production of fecal pellets (towards the small N detritus pool).

The zooplankton equation expressed in carbon is:

$$\frac{\partial\text{Zoo}}{\partial t} \Big|_C = \text{CN}_p g\beta\text{Zoo} - \text{CN}_z \left[\left(l_{\text{BM}} + l_{\text{E}} \beta \frac{g}{g_{\text{max}}} \right) \text{Zoo} - m_z\text{Zoo}^2 \right] - r_{\text{Cexc}}\text{CN}_z\text{Zoo}$$

where r_{Cexc} is the rate of carbon excess respiration due to the C–N ratio difference between phytoplankton and zooplankton. The constant zooplankton C–N ratio ($\text{CN}_z = 5.0$) leads to the formulation: $\text{CN}_z = (\text{CN}_p\beta g\text{Zoo} - r_{\text{Cexc}}\text{CN}_z\text{Zoo})/\beta g\text{Zoo}$

or

$$r_{\text{Cexc}} = \beta g(\text{CN}_p - \text{CN}_z)/\text{CN}_z$$

This excess of respired organic carbon is directed to DIC. It ensures the conservation of the zooplankton C–N ratio and therefore the zooplankton equation expressed in carbon is implicit.

DIC

The air–sea exchange of carbon dioxide is taken from Fennel et al. (2008).

- $\partial\text{DIC}/\partial t =$ –Nutrient-based uptake by phytoplankton growth
- C excess-based semi-labile DOC exudation
 - + Nutrient-based exudation of labile DOC
 - + Labile DOC produced by sloppy feeding
 - + Excretion (basal metabolism and grazing dependent)
 - + Solubilization small and large detritus C (labile fraction)
 - + Remineralization of semi-labile DOC + Air–sea CO_2 flux

$$\begin{aligned} \frac{\partial\text{DIC}}{\partial t} = & \text{CN}_p(-\mu\text{Phy} - \gamma\sigma_C\mu_{\text{max}}L_L(1 - L_N)\text{Phy} + \omega_C\mu\text{Phy} \\ & + (1 - \beta)Q_{\text{DOC}}(1 - \delta_C)g\text{Zoo}) + \dots + \text{CN}_z \left(l_{\text{BM}} + l_{\text{E}}\beta\frac{g}{g_{\text{max}}} \right. \\ & \left. + r_{\text{Cexc}} \right) \text{Zoo} + S_{\text{SDetC}}\text{SDetC} + S_{\text{LDetC}}\text{LDetC} \\ & + a_{\text{CO}}e^{0.07T}\text{DOC} + \dots + \frac{vK_{\text{CO}_2}\text{CO}_{2,\text{sol}}(p\text{CO}_{2,\text{air}} - p\text{CO}_2)}{\Delta z} \end{aligned}$$

Ammonium

- $\partial\text{NH}_4/\partial t =$ –Ammonium uptake by phytoplankton growth
- + Exudation of labile DON
 - + Labile DON produced by sloppy feeding
 - + Excretion (basal metabolism and grazing dependent)
 - + Solubilization small and large detritus N (labile fraction)
 - + Remineralization of semi-labile DON – Nitrification

$$\begin{aligned} \frac{\partial\text{NH}_4}{\partial t} = & -\mu_{\text{max}}L_L L_{\text{NH}_4}\text{Phy} + \omega_N\mu\text{Phy} \\ & + (1 - \beta)Q_{\text{DON}}(1 - \delta_N)g\text{Zoo} + \left(l_{\text{BM}} + l_{\text{E}}\beta\frac{g}{g_{\text{max}}} \right) \text{Zoo} \\ & + \dots + (1 - \delta_N)(S_{\text{SDetN}}\text{SDetN} + S_{\text{LDetN}}\text{LDetN}) \\ & + a_{\text{NO}}e^{0.07T}\text{DON} - n\text{NH}_4 \end{aligned}$$

where l_{BM} and l_{E} are the zooplankton excretion rates due to basal metabolism and assimilation intensity respectively, and n is the nitrification rate (same parameterization than in Fennel et al. (2006)). L_L is the non-dimensional light limitation and L_{NH_4} is the nutrient limitation term for ammonium.

Nitrate

- $\partial\text{NO}_3/\partial t =$ –Nitrate uptake by phytoplankton growth
- + Nitrification

$$\frac{\partial \text{NO}_3}{\partial t} = -\mu_{\max} L_L L_{\text{NO}_3} \text{Phy} + n \text{NH}_4$$

where L_{NO_3} is the nutrient limitation term for nitrate.

Detritus N

$\partial \text{SDetN} / \partial t$ = Phytoplankton mortality
 – Aggregation with living phytoplankton cells
 – Small detritus N solubilization
 – Sinking of small detritus N

$$\frac{\partial \text{SDetN}}{\partial t} = m_p \text{Phy} - \tau (\text{SDetN} + \text{Phy}) \text{SDetN} - s_{\text{SDetN}} \text{SDetN} - w_s \frac{\partial \text{SDetN}}{\partial z}$$

$\partial \text{LDetN} / \partial t$ = Fecal pellets production (nitrogen fraction)
 + Zooplankton mortality
 + Aggregation of small detritus (N) and phytoplankton cells
 – Large detritus N solubilization
 – Sinking of large detritus (N)

$$\frac{\partial \text{LDetN}}{\partial t} = (1 - \beta)(1 - Q_{\text{DON}})g_{\text{Zoo}} + m_z \text{Zoo}^2 + \tau (\text{SDetN} + \text{Phy})^2 - s_{\text{LDetN}} \text{LDetN} - w_L \frac{\partial \text{LDetN}}{\partial z}$$

Detritus C

$\partial \text{SDetC} / \partial t$ = Phytoplankton mortality (C)
 – Aggregation with living phytoplankton cells
 – Small detritus C remineralization
 – Sinking of small detritus C

$$\frac{\partial \text{SDetC}}{\partial t} = \text{CN}_p m_p \text{Phy} - \tau (\text{SDetC} + \text{CN}_p \text{Phy}) \text{SDetC} - s_{\text{SDetC}} \text{SDetC} - w_s \frac{\partial \text{SDetC}}{\partial z}$$

$\partial \text{POC}_L / \partial t$ = Fecal pellets production (carbon)
 + Zooplankton mortality (C)
 + Aggregation of small detritus (C) and phytoplankton cells (C)
 – Large detritus C solubilization
 – Sinking of large detritus (C)

$$\frac{\partial \text{LDetC}}{\partial t} = \text{CN}_p (1 - \beta)(1 - Q_{\text{DOC}})g_{\text{Zoo}} + \text{CN}_z m_z \text{Zoo}^2 + \tau (\text{SDetC} + \text{CN}_p \text{Phy})^2 - s_{\text{LDetC}} \text{LDetC} + \dots - w_L \frac{\partial \text{LDetC}}{\partial z}$$

where w_s and w_L are the sinking velocities of small and large detritus respectively.

Bottom boundary condition

In order to take into account the resuspension of detritus C near the seabed due to bottom friction, a fraction (λ_{res} , see next section) of the bottom carbon flux is resuspended and mineralized in the lower water column. The complementary fraction ($1 - \lambda_{\text{res}}$) is buried, the flux of buried carbon thus is:

$$F_{\text{Cburied}} = \text{BE}_C (1 - \lambda_{\text{res}}) F_{\text{Cbottom}}$$

where BE_C is the burial efficiency (see next section) and F_{Cbottom} is the detritus C flux that reaches the bottom before resuspension:

$$F_{\text{Cbottom}} = \text{CN}_p w_p \frac{\partial \text{Phy}}{\partial z} \Big|_{z=H} + w_s \frac{\partial \text{SDetC}}{\partial z} \Big|_{z=H} + w_L \frac{\partial \text{LDetC}}{\partial z} \Big|_{z=H}$$

The POM which is not resuspended nor buried is mineralized and therefore the bottom boundary condition for carbon follows:

$\partial \text{DIC} / \partial t \Big|_{z=H}$ = mineralization of (resuspended bottom detritus C + not resuspended nor buried bottom POC)

$$\frac{\partial \text{DIC}}{\partial t} \Big|_{z=H} = F_{\text{Cbottom}} (\lambda_{\text{res}} + (1 - \lambda_{\text{res}})(1 - \text{BE}_C))$$

For nitrogen, the same resuspension rate is applied (λ_{res}) to the detritus N reaching the seabed. The remaining detritus N is subject to burial and denitrification following:

$$F_{\text{Nresuspended}} = \lambda_{\text{res}} F_{\text{Nbottom}} \\ F_{\text{Nburied}} = \text{BE}_N (1 - \lambda_{\text{res}}) F_{\text{Nbottom}} \\ F_{\text{Ndenitrified}} = (1 - \text{BE}_N)(1 - \lambda_{\text{res}}) F_{\text{Nbottom}}$$

where F_{Nbottom} is the flux of detritus in nitrogen that reaches the bottom before resuspension:

$$F_{\text{Nbottom}} = w_p \frac{\partial \text{Phy}}{\partial z} \Big|_{z=H} + w_s \frac{\partial \text{SDetN}}{\partial z} \Big|_{z=H} + w_L \frac{\partial \text{LDetN}}{\partial z} \Big|_{z=H}$$

The denitrification process is taken into account as it was shown to be significant in the MAB (Fennel et al., 2006). The stoichiometry calculation shows that the bottom boundary condition for ammonium is:

$\partial \text{NH}_4 / \partial t \Big|_{z=H}$ = mineralization of (resuspended bottom detritus N + not resuspended nor buried bottom detritus N + not resuspended nor denitrified bottom detritus N)

$$\frac{\partial \text{NH}_4}{\partial t} \Big|_{z=H} = F_{\text{Nresuspended}} + \frac{4}{16} F_{\text{Ndenitrified}} \\ \frac{\partial \text{NH}_4}{\partial t} \Big|_{z=H} = (\lambda_{\text{res}} + \frac{4}{16}(1 - \lambda_{\text{res}})(1 - \text{BE}_N)) F_{\text{Nbottom}}$$

The total amount of nitrogen lost through burial and denitrification (N_2) is:

$$F_{\text{Nlost}} = F_{\text{Nburied}} + \frac{12}{16} F_{\text{Ndenitrified}} \\ F_{\text{Nlost}} = \frac{4}{16} (1 - \lambda_{\text{res}}) (3 + \text{BE}_N) F_{\text{Nbottom}}$$

The POM resuspension. The resuspension is taken into account as a function of the friction velocity at the seabed (U^*). The resuspension rate (%) follows:

$$\lambda_{\text{res}} = \frac{(U^*)^2}{(U_d^*)^2}$$

where U_d^* is the critical friction velocity above which all organic matter is maintained in suspension ($U_d^* = 0.31 \text{ cm s}^{-1}$, Peterson, 1999). The resuspended fraction of POC is thus largely dependent on the local near bottom current velocity which is driven by the general circulation and the tides on the continental shelf and also by wind events in shallow waters.

The POM burial. Thomas et al. (2002) measured and reviewed high rates of carbon burial along the continental shelf of the U.S. north-eastern continental shelf. The carbon and nitrogen burial rates have been implemented to simulate the loss of material in the sediment.

A fraction (burial efficiency, BE_C) of the particulate organic carbon that reaches the seabed is buried following the empirical expression of Henrichs and Reeburgh (1987):

$$\log Fc = 0.69 \log w + 2.27$$

and

$$BE_C = w^{0.4} / 2.1$$

where Fc is the organic carbon flux at the sediment surface ($gC\ m^{-2}\ y^{-1}$) and w is the sediment accumulation rate ($cm\ y^{-1}$). Resolving the system leads to the following formulation for BE_C (%):

$$BE_C = \frac{1}{2.1} \left[10^{\left(\frac{\log Fc}{0.69} - 2.27 \right)} \right]^{0.4}$$

This formulation matches the upper values of Thomas et al. (2002) who measured and reviewed burial efficiency values (in % of organic carbon deposition): 10–20% at the slope off Cape Cod (SEEP-I), 25–50% in the MAB (SEEP-II) = 25–50, 3–40% at the slope off Cape Hatteras.

C–N ratios of buried organic matter of 9–10 were reported for the shelf and estuarine surface sediments and slightly lower in deeper waters (Gelinis et al., 2001). A value of $CN_{burial} = 9.3$ is used to estimate the flux of buried organic nitrogen in agreement with values measured in the sediment of the MAB shelf (Mayer et al., 2002; Mayer, pers. comm.).

A maximum of 75% of carbon burial efficiency is applied as it corresponds to the maximum value measured:

$$BE_C = \text{MIN} \{ [10(\log Fc / 0.69 - 2.27)]^{0.4} / 2.1; 0.75 \}$$

For nitrogen burial, a similar expression of burial efficiency is used introducing a CN_{burial} ratio:

$$BE_N = \text{MIN} \left\{ \left[10^{(\log(CN_{burial} FN) / 0.69 - 2.27)} \right]^{0.4} / 2.1; 0.75 \right\}$$

References

Admiraal, W., Peletier, H., Lane, R., 1986. Nitrogen metabolism of marine planktonic diatoms; excretion, assimilation and cellular pools of free amino acids in seven species with different cell size. *Journal of Experimental Marine Biology and Ecology* 98, 241–263.

Aluwihare, L., Repeta, D., Chen, R., 2002. Chemical composition and cycling of dissolved organic matter in the Mid-Atlantic Bight. *Deep Sea Research* 49, 4421–4437.

Amon, R., Benner, R., 1996. Bacterial utilization of different size classes of dissolved organic matter. *Limnology and Oceanography* 41, 41–51.

Anderson, T., Pondaven, P., 2003. Non-redfield carbon and nitrogen cycling in the Sargasso Sea: pelagic imbalances and export flux. *Deep Sea Research Part I: Oceanographic Research Papers* 50, 573–591.

Anderson, T., Williams, P., 1998. Modelling the seasonal cycle of dissolved organic carbon at station E1 in the English Channel. *Estuarine, Coastal and Shelf Science* 46, 93–109.

Baines, S., Pace, M., 1991. The Production of dissolved organic matter by phytoplankton and its importance to bacteria: patterns across marine and freshwater systems. *Limnology and Oceanography* 36, 1078–1090.

Bates, N., Hansell, D., 1999. A high resolution study of surface layer hydrographic and biogeochemical properties between Chesapeake Bay and Bermuda. *Marine Chemistry* 67, 1–16.

Bauer, J., Druffel, E., 1998. Ocean margins as a significance source of organic matter to the open ocean. *Nature* 392, 482–485.

Bauer, J.E., Druffel, E.R.M., Wolgast, D.M., Griffin, S., 2001. Cycling of dissolved and particulate organic radiocarbon in the northwest Atlantic continental margin. *Global Biogeochemical Cycles* 15, 615–636.

Bauer, J.E., Druffel, E.R.M., Wolgast, D.M., Griffin, S., 2002. Temporal and regional variability in sources and cycling of DOC and POC in the northwest Atlantic continental shelf and slope. *Deep Sea Research* 49, 4387–4419.

Beardsley, R., Boicourt, W., 1981. On estuarine and continental shelf circulation in the Middle Atlantic Bight. *Evolution of Physical Oceanography*, 198–233.

Benner, R., Pakulski, J., McCarthy, M., Hedges, J., Hatcher, P., 1992. Bulk chemical characteristics of dissolved organic matter in the ocean. *Science* 255, 1561.

Berger, W., 1989. *Global Maps of Ocean Productivity*. Productivity of the Oceans: Present and Past. Wiley, New York, pp. 429–455.

Biddanda, B., Benner, R., 1997. Carbon, nitrogen, and carbohydrate fluxes during the production of particulate and dissolved organic matter by marine phytoplankton. *Limnology and Oceanography* 42, 506–518.

Biscaye, P., Anderson, R., 1994. Fluxes of particulate matter on the slope of the southern Middle Atlantic Bight: SEEP-II. *Deep Sea Research Part II: Topical Studies in Oceanography* 41, 459–509.

Biscaye, P., Anderson, R., Deck, B., 1988. Fluxes of particles and constituents to the eastern United States continental slope and rise: SEEP-I. *Continental Shelf Research* 8, 855–904.

Biscaye, P., Flagg, C., Falkowski, P., 1994. The shelf edge exchange processes experiment, SEEP-II: an introduction to hypotheses, results and conclusions. *Deep Sea Research Part II: Topical Studies in Oceanography* 41, 231–252.

Bjornsen, B., 1988. Phytoplankton exudation of organic matter: why do healthy cells do it. *Limnology and Oceanography* 33, 151–154.

Bronk, D., Glibert, P., Ward, B., 1994. Nitrogen uptake, dissolved organic nitrogen release, and new production. *Science* 265, 1843.

Bronk, D., Ward, B., 2000. Magnitude of dissolved organic nitrogen release relative to gross nitrogen uptake in marine systems. *Limnology and Oceanography* 45, 1879–1883.

Brush, M., Brawley, J., Nixon, S., Kremer, J., 2002. Modeling phytoplankton production: problems with the Eppley curve and an empirical alternative. *Marine Ecology Progress Series* 238, 31–45.

Carlson, C., 2002. Production and Removal Processes. *Biogeochemistry of Marine Dissolved Organic Matter*. Academic, pp. 91–151.

Chen, R.F., Fry, B., Hopkinson, C.S., Repeta, D.J., Peltzer, E.T., 1996. Dissolved organic carbon on Georges Bank. *Continental Shelf Research* 16, 409–420.

DeGrandpre, M., Olbu, G., Beatty, C., Hammar, T., 2002. Air–sea CO_2 fluxes on the US Middle Atlantic Bight. *Deep Sea Research Part II: Topical Studies in Oceanography* 49, 4355–4367.

Dinniman, M., Klinck, J., Smith, W., 2003. Cross-shelf exchange in a model of the Ross Sea circulation and biogeochemistry. *Deep Sea Research Part II: Topical Studies in Oceanography* 50, 3103–3120.

Druffel, E., Williams, P., Bauer, J., Ertel, J., 1992. Cycling of dissolved and particulate organic matter in the open ocean. *Journal of Geophysical Research* 97, 15639–15659.

Eppley, R., 1972. Temperature and phytoplankton growth in the sea. *Fishery Bulletin* 70, 1063–1085.

Fairall, C., Bradley, E., Hare, J., Grachev, A., Edson, J., 2003. Bulk parameterization of air–sea fluxes: updates and verification for the COARE algorithm. *Journal of Climate* 16, 571–591.

Falkowski, P., Flagg, C., Rowe, G., Smith, S., Whitley, T., Wirick, C., 1988. The fate of a spring phytoplankton bloom: export or oxidation. *Continental Shelf Research* 8, 457–484.

Fasham, M., Boyd, P., Savidge, G., 1999. Modeling the relative contributions of autotrophs and heterotrophs to carbon flow at a Lagrangian JGOFS Station in the Northeast Atlantic: the importance of DOC. *Limnology and Oceanography* 44, 80–94.

Fennel, K., Wilkin, J., Levin, J., Moisan, J., O'Reilly, J., Haidvogel, D., 2006. Nitrogen cycling in the Middle Atlantic Bight: results from a three-dimensional model and implications for the North Atlantic nitrogen budget. *Global Biogeochemical Cycles* 20.

Fennel, K., Wilkin, J., Previdi, M., Najjar, R., 2008. Denitrification effects on air–sea CO_2 flux in the coastal ocean: simulations for the northwest North Atlantic. *Geophysical Research Letters* 35.

Fisher, T.S., Hagy, J.D., Rochelle-Newall, E., 1998. Dissolved and particulate organic carbon in Chesapeake Bay. *Estuaries* 21, 215–229.

Flather, R., 1976. A tidal model of the northwest European continental shelf. *Mémoires de la Société Royale des Sciences de Liège* 6, 141–164.

Fogg, G., 1966. The extracellular products of algae. *Oceanography and Marine Biology: an Annual Review* 4, 195–212.

Fogg, G., 1983. The ecological significance of extracellular products of phytoplankton photosynthesis. *Botanica Marina* 26, 3–14.

Geider, R., MacIntyre, H., Kana, T., 1997. Dynamic model of phytoplankton growth and acclimation: responses of the balanced growth rate and the chlorophyll a: carbon ratio to light, nutrient-limitation and temperature. *Marine Ecology Progress Series* 148, 187–200.

Gelinis, Y., Baldock, J., Hedges, J., 2001. Organic carbon composition of marine sediments: effect of oxygen exposure on oil generation potential. *Science* 294, 145–148.

Haidvogel, D., Arango, H., Hedstrom, K., Beckmann, A., Malanotte-Rizzoli, P., Shchepetkin, A., 2000. Model evaluation experiments in the North Atlantic Basin: simulations in nonlinear terrain-following coordinates. *Dynamics of Atmospheres and Oceans* 32, 239–281.

Haidvogel, D.B., Arango, H., Budgell, W.P., Cornuell, B.D., Curchitser, E., 2008. Regional ocean forecasting in terrain-following coordinates: model formulation and skill assessment. *Journal of Computational Physics*.

Hansell, D., 2002. In: Hansell, D., Carlson, C. (Eds.), *Biogeochemistry of Marine Dissolved Organic Matter*. Academic Press, New-York, pp. 685–716.

Harvey, H., Mannino, A., 2001. The chemical composition and cycling of particulate and macromolecular dissolved organic matter in temperate estuaries as revealed by molecular organic tracers. *Organic Geochemistry* 32, 527–542.

Harvey, H., Tuttle, J., Bell, J., 1995. Kinetics of phytoplankton decay during simulated sedimentation: changes in biochemical composition and microbial activity under oxic and anoxic conditions. *Geochimica et Cosmochimica Acta* 59, 3367–3377.

Hasegawa, T., Koike, I., Mukai, H., 2001. Fate of food nitrogen in marine copepods. *Marine Ecology Progress Series* 210, 167–174.

- Hellebust, J., 1965. Excretion of Some organic compounds by marine phytoplankton. *Limnology and Oceanography* 10, 192–206.
- Henrichs, S., Reeburgh, W., 1987. Anaerobic mineralization of marine sediment organic matter: rates and the role of anaerobic processes in the oceanic carbon economy. *Geomicrobiology Journal* 5 (3/4), 191–237. <http://www.informaworld.com/smppt/title%7Edb=all%7Econtent=t713722957>.
- Hofmann, E., Druon, J.N., Fennel, K., Friedrichs, M., Haidvogel, D., Lee, C., Mannino, A., McClain, C., Najjar, R., O'Reilly, J., Pollard, D., Previdi, M., Seitzinger, S., Siewert, S., Signorini, S., Wilkin, J., 2008. Eastern U.S. continental shelf carbon budget: integrating models, data assimilation, and analysis. *Oceanography* 21, 86–104.
- Hopkinson, C., Fry, B., Nolin, A., 1997. Stoichiometry of dissolved organic matter dynamics on the continental shelf of the northeastern USA. *Continental Shelf Research* 17, 473–489.
- Hopkinson, C.S., Vallino, J.J., Nolin, A., 2002. Decomposition of dissolved organic matter from the continental margin. *Deep Sea Research Part II: Topical Studies in Oceanography* 49, 4461–4478.
- Ianson, D., Allen, S., 2002. A two-dimensional nitrogen and carbon flux model in a coastal upwelling region. *Global Biogeochemical Cycles* 16, 1011.
- Jensen, L., 1983. Phytoplankton release of extracellular organic carbon, molecular weight composition, and bacterial assimilation. *Marine Ecology Progress Series* 11, 39–48.
- Jolliff, J.K., Kindle, J.C., Shulman, I., Penta, B., Friedrichs, M.A.M., Helber, R., Arnone, R. A., 2009. Summary diagrams for coupled hydrodynamic-ecosystem model skill assessment. *Journal of Marine Systems* 76, 64–82.
- Kantha, L., Clayson, C., 1994. An improved mixed layer model for geophysical applications. *Journal of Geophysical Research* 99, 25235–25266.
- Lancelot, C., 1983. Factors affecting phytoplankton extracellular release in the Southern Bight of the North Sea. *Marine Ecology Progress Series* 12, 115–121.
- Lancelot, C., 1984. Extracellular release of small and large molecules by phytoplankton in the southern Bight of the North Sea. *Estuarine, Coastal and Shelf Science* 18, 65–77.
- Lancelot, C., Billen, G., 1985. Carbon-nitrogen relationships in nutrient metabolism of coastal marine ecosystems. *Advances in Aquatic Microbiology* 3, 263–321.
- Lancelot, C., Spitz, Y., Gypens, N., Ruddick, K., Becquevort, S., Rousseau, V., Lacroix, G., Billen, G., 2005. Modelling diatom and *Phaeocystis* blooms and nutrient cycles in the Southern Bight of the North Sea: the MIRO model. *Marine Ecology Progress Series* 289, 63–78.
- Ledwell, J., Watson, A., Law, C., 1993. Evidence for slow mixing across the pycnocline from an open-ocean tracer-release experiment. *Nature* 364, 701–703.
- Magnuson, A., Harding, L., Mallonee, M., Adolf, J., 2004. Bio-optical model for Chesapeake bay and the Middle Atlantic Bight. *Estuarine, Coastal and Shelf Science*.
- Mannino, A., 2000. Chemical Composition of Particulate and Macromolecular Dissolved Organic Matter in the Delaware Estuary and Experimental Diatom Blooms: Sources and Reactivity Patterns. Marine, Estuarine, Environmental Sciences Graduate Program, University of Maryland, College Park.
- Mannino, A., Harvey, H.R., 2000. Biochemical composition of particles and dissolved organic matter along an estuarine gradient: sources and implications for DOM reactivity. *Limnology and Oceanography* 45, 775–788.
- Mannino, A., Russ, M.E., Hooker, S.B., 2008. Algorithm development and validation for satellite-derived distributions of DOC and CDOM in the US Middle Atlantic Bight. *Journal of Geophysical Research* 113, C07051. doi:10.1029/2007JC004493.
- Marañón, E., Cermeno, P., Fernandez, E., Rodriguez, J., Zabala, L., 2004. Significance and mechanisms of photosynthetic production of dissolved organic carbon in a coastal eutrophic ecosystem. *Limnology and Oceanography* 49, 1652–1666.
- Marchesiello, P., McWilliams, J., Shchepetkin, A., 2003. Equilibrium structure and dynamics of the California current system. *Journal of Physical Oceanography* 33, 753–783.
- Mayer, L., Benninger, L., Bock, M., DeMaster, D., Roberts, Q., Martens, C., 2002. Mineral associations and nutritional quality of organic matter in shelf and upper slope sediments off Cape Hatteras, USA: a case of unusually high loadings. *Deep Sea Research Part II: Topical Studies in Oceanography* 49, 4587–4597.
- Mellor, G., Yamada, T., 1982. Development of a turbulence closure model for geophysical fluid problems. *Reviews of Geophysics and Space Physics* 20, 851–875.
- Møller, E., 2005. Sloppy feeding in marine copepods: prey-size-dependent production of dissolved organic carbon. *Journal of Plankton Research* 27, 27.
- Møller, E., Thor, P., Nielsen, T., 2003. Production of DOC by *Calanus finmarchicus*, *C. glacialis* and *C. hyperboreus* through sloppy feeding and leakage from fecal pellets. *Marine Ecology Progress Series* 262, 185–191.
- Mouw, C., Yoder, J., 2005. Primary production calculations in the Mid-Atlantic Bight, including effects of phytoplankton community size structure. *Limnology and Oceanography* 50, 1232–1243.
- Nagata, T., 2000. In: Kirchman, D. (Ed.), *Microbial Ecology of the Oceans*. Wiley, New-York, pp. 121–152.
- Norrman, B., Zweifel, U., Hopkinson Jr., C., Fry, B., 1995. Production and utilization of dissolved organic carbon during an experimental diatom bloom. *Limnology and Oceanography* 40, 898–907.
- O'Reilly, J., Busch, D., 1984. Phytoplankton primary production on the northwestern Atlantic shelf. *Rapports et Procès-Verbaux des Réunions du Conseil International pour l'Exploration de la Mer* 183, 255–268.
- O'Reilly, J., Evans-Zetlin, C., Busch, D., 1987. In: Backus, R. (Ed.), *Georges Bank*. MIT Press, Cambridge, MA, pp. 220–233.
- Obernosterer, I., Herndl, G., 1995. Phytoplankton extracellular release and bacterial growth: dependence on the inorganic N:P ratio. *Marine Ecology Progress Series* 116, 247–257.
- Peliz, A., Dubert, J., Haidvogel, D., Le Cann, B., 2003. Generation and unstable evolution of a density-driven eastern poleward current: the Iberian Poleward Current. *Journal of Geophysical Research* 108, 3268.
- Peterson, E., 1999. Benthic shear stress and sediment condition. *Aquacultural Engineering* 21, 85–111.
- Ploug, H., Grossart, H., 2000. Bacterial growth and grazing on diatom aggregates: respiratory carbon turnover as a function of aggregate size and sinking velocity. *Limnology and Oceanography* 45, 1467–1475.
- Pomeroy, L., Wiebe, W., Deibel, D., Thompson, R., Rowe, G., Palkulski, J., 1991. Bacterial responses to temperature and substrate concentration during the Newfoundland spring bloom. *Marine Ecology Progress Series* 75, 143–159.
- Popova, E.E., Anderson, T.R., 2002. Impact of including dissolved organic matter in a global ocean box model on simulated distributions and fluxes of carbon and nitrogen. *Geophysical Research Letters* 29 (9), 1303. doi:10.1029/2001GL014274. <http://www.agu.org/pubs/crossref/2002.../2001GL014274.shtml>.
- Raick, C., Delhez, E., Soetaert, K., Gregoire, M., 2005. Study of the seasonal cycle of the biogeochemical processes in the Ligurian Sea using a 1D interdisciplinary model. *Journal of Marine Systems*.
- Redalje, D., Lohrenz, S., Verity, P., Flagg, C., 2002. Phytoplankton dynamics within a discrete water mass off Cape Hatteras, North Carolina: the Lagrangian experiment. *Deep Sea Research Part II: Topical Studies in Oceanography* 49, 4511–4531.
- Ryan, J., Yoder, J., Cornillon, P., 1999. Enhanced chlorophyll at the Shelfbreak of the Mid-Atlantic Bight and Georges Bank during the spring transition. *Limnology and Oceanography* 44, 1–11.
- Sambrotto, R., Savidge, G., Robinson, C., Boyd, P., Takahashi, T., Karl, D., Langdon, C., Chipman, D., Marra, J., Codispoti, L., 1993. Elevated consumption of carbon relative to nitrogen in the surface ocean. *Nature* 363, 248–250.
- Santschi, P., Guo, L., Baskaran, M., Trumbore, S., Southon, J., Bianchi, T., Honeyman, B., Cifuentes, L., 1995. Isotopic evidence for the contemporary origin of high-molecular weight organic matter in oceanic environments. *Geochimica et Cosmochimica Acta* 59, 625–631.
- Schaff, T., Levin, L., Blair, N., DeMaster, D., Pope, R., Boehme, S., 1992. Spatial heterogeneity of benthos on the Carolina continental slope: large (100 km)-scale variation. *Marine Ecology Progress Series* 88, 143–160.
- Schollaert, S., Rossby, T., Yoder, J., 2003. Gulf Stream cross-frontal exchange: possible mechanisms to explain interannual variations in phytoplankton chlorophyll in the Slope Sea during the SeaWiFS years. *Deep Sea Research*.
- Seitzinger, S., Sanders, R., 1999. Atmospheric inputs of dissolved organic nitrogen stimulate estuarine bacteria and phytoplankton. *Limnology and Oceanography* 44, 721–730.
- Sharp, J., Culbertson, C., Church, T., 1982. The chemistry of the Delaware estuary. General considerations. *Limnology and Oceanography* 27, 1015–1028.
- Six, K., Maier-Reimer, E., 1996. Effects of plankton dynamics on seasonal carbon fluxes in an ocean general circulation model. *Global Biogeochemical Cycles* 10, 559–583.
- Smith, D., Simon, M., Alldredge, A., Azam, F., 1992. Intense hydrolytic enzyme activity on marine aggregates and implications for rapid particle dissolution. *Nature* 359, 139–142.
- Søndergaard, M., Williams, P., Cauwet, G., Riemann, B., Robinson, C., Terzic, S., Woodward, E., Worm, J., 2000. Net accumulation and flux of dissolved organic carbon and dissolved organic nitrogen in marine plankton communities. *Limnology and Oceanography* 45, 1097–1111.
- Taylor, G.T., Way, J., Scraton, M.L., 2003. Planktonic carbon cycling and transport in surface waters of the highly urbanized Hudson River estuary. *Limnology and Oceanography* 48, 1779–1795.
- Thingstad, T., Hagström, A., Rassoulzadegan, F., 1997. Accumulation of degradable DOC in surface waters: is it caused by a malfunctioning microbial loop? *Limnology and Oceanography* 42, 398–404.
- Thomas, C., Blair, N., Alperin, M., DeMaster, D., Jahnke, R., Martens, C., Mayer, L., 2002. Organic carbon deposition on the North Carolina continental slope off Cape Hatteras (USA). *Deep Sea Research Part II: Topical Studies in Oceanography* 49, 4687–4709.
- Varela, M., Barquero, S., Bode, A., Fernandez, E., Gonzalez, N., Teira, E., Varela, M., 2003. Microplanktonic regeneration of ammonium and dissolved organic nitrogen in the upwelling area of the NW of Spain: relationships with dissolved organic carbon production and phytoplankton size-structure. *Journal of Plankton Research* 25, 719.
- Verity, P., Redalje, D., Lohrenz, S., Flagg, C., Hristov, R., 2002. Coupling between primary production and pelagic consumption in temperate ocean margin pelagic ecosystems. *Deep Sea Research Part II: Topical Studies in Oceanography* 49, 4553–4569.
- Vlahos, P., Chen, R.F., Repeta, D.J., 2002. Dissolved organic carbon in the Mid-Atlantic Bight. *Deep Sea Research Part II: Topical Studies in Oceanography* 49, 4369–4385.
- Walsh, J., 1994. Particle export at Cape Hatteras. *Deep Sea Research Part II: Topical Studies in Oceanography* 41, 603–628.
- Warner, J., Sherwood, C., Arango, H., Signell, R., 2005. Performance of four turbulence closure models implemented using a generic length scale method. *Ocean Modelling* 8, 81–113.
- Wilkin, J., 2006. The summertime heat budget and circulation of Southeast New England shelf waters. *Journal of Physical Oceanography* 36, 1997–2011.
- Williams, P., 1990. The importance of losses during microbial growth: commentary on the physiology, measurement and ecology of the release of dissolved organic material. *Marine Microbial Food Webs* 4, 175–206.